RESPONSES TO REVIEWERS

Formatted: Font: Bold

Formatted: Centered

Anonymous Referee #1

General comments: This manuscript reported modeling impacts of nitrification inhibitor (NI) application on N2O emission. The authors incorporated new processes into the ecosys model and compared the simulations against field observations and some literature reports. In general, the work in this manuscript can contribute to the simulations of NI impacts on N2O production and emission. However, I think some changes can further improve this manuscript.

Firstly, the new contents in this manuscript are simulating NI impacts and a lot of descriptions in the section 2 (model development) are the introductions of the ecosys model, instead of the new model development. These introductions are not necessary for me since they have been well described in literatures. I suggest the authors delete unnecessary descriptions (or move them into supporting materials) and focus more on the new model improvement/new contents.

I have reworded sec. 2.1 to clarify the relationship between the description of earlier model components in sec. 2.2 to 2.8, and nitrification inhibition in sec. 2.9. However because readers' understanding sec. 2.9 requires their understanding of sec. 2.2 to 2.8, I am reluctant to abbreviate them, as I frequently refer to specific steps in these sections to explain model behavior in the Discussion. I have removed Sec. 2.10 and 2.11, and all later references to them, to shorten the manuscript.

Secondly, I have noticed some discrepancies between simulations and observations in yields, mineral nitrogen, and N2O emission. However, some discrepancies were not fully discussed. I would like to see more discussions regarding what might be reasons for the discrepancies and how the discrepancies (and reasons) inform further improvement in simulating N2O emission following soil thaw and NI impacts.

I have added Sec. 6.5 to the Discussion in which I raise ongoing issues about modelling N2O emissions and NI effects on them. I have confined this section to these issues as they are the focus of this paper, rather than mineral N and crop yields.

Specific comments:
Lines 96 to 99: This sentence is not clear for me. Please rewrite.

Done

Line 230: From this section, it seems that impacts of NI are not related to the application amount of NI. Is this reasonable? Does this need to be considered in further model developments.

I have not seen any experimental results in the literature in which different amounts of NI were evaluated from which such an impact could be parameterized. I have added a note to this effect in Sec. 6.4.

Line 235: "Itl" in the right part should be "I(t-1)l"?

Good point. Done

Line 311: So the measurement depths were shallower than the depth of slurry injection? Is this a potential reason for the discrepancies between the simulated and observed mineral nitrogen.

That could be, because the mineral N would have to diffuse upwards from the injection zone.

Line 324: "as soon as possible" may be not proper here.

Reworded in Sec. 3.2

Line 346: Could you clarify the source of the parameters in the Table 2? All from field records?

Ksat was derived from a pedotransfer function, as now noted in Table 2. All others are from field records.

Line 354: Could you provide the input parameters of the simulated crop?

That would require a lot more model explanation that has already been provided in earlier papers, and would be inconsistent with the first point about shortening the model description raised above. Also crop growth is not the key focus of this paper, but rather NI.

Line 372: Did you mean disturbance of the soil profile from surface to 0.5m or 0.8m? If so, is this setting accommodate to normal tillage practices? Is 0.8m too deep?

These values refer to soil mixing coefficients during tillage, not depth which was that of application (14 cm) as stated in Sec. 4.2.

Lines 421 to 422: This sentence is hard to follow. Could you rewrite into two short sentences?

This sentence is already less than 2 lines.

Line 469: RI should be NI? Please check other places of the manuscript.

Reworded in Sec. 5.4.1 to show that R_I refers to rate constants for declining NI activity used for DMPP and nitrapyrin.

Line 473: Deleting "and measured" as these are modeled values.

This line refers to Table 5 that shows both modelled and measured values.

Line 534: Could you please discuss more about the discrepancies in simulating yields in this section, such as the reasons and implications for further model improvement.

That would be interesting, but the point most relevant to this paper is whether NI affected modelled and measured barley yields. In common with most NI studies, yields were not much affected. I mentioned that yields were reduced by lodging in the 2016 field experiment.

Line 567: How about N2O reduction to N2 during this period? Was the rate of this process low or high?

This process is modelled in ecosys, but no experimental data are available from this study to corroborate modelled values.

Line 606: Should be "Lin et al., 2018".

Corrected

Line 632: grammar error.

I split this sentence in Sec. 6.2.1 to simplify the grammar.

Line 693: more intensive tillage could accelerate O2 transfer from atmosphere to soils. Does the model consider this?

Yes, but I thought this was getting too detailed for a discussion of NI effects.

Line 736: May be the offset need to considered not only in Tier 3 methodology but also other methodologies.

Perhaps, but measurements of this offset are limited.

Figure 3a, b: O2 were zero for about 10 days. Did the model simulate N2O reduction to N2 during this period?

Actually O2 was not zero, but very near zero. N2O reduction can be modelled, depending on demand for e- acceptors unmet by NO3-, NO2- and N2O. N2 emissions from N2O reduction are modelled in ecosys, but were not included in this paper.

Figures 4 to 7: Did you compare daily simulations against daily observations? It looks that the auto-chamber observations were sub-daily; if so, how many observations per day? It would be useful to clarity these points.

Observed fluxes were plotted at the same 3-h frequency as that at which they were measured as now stated in Sec. 3.2.

Anonymous Referee #2

The authors have modified the ecosystem model to simulate effects of nitrification inhibitors on N2O emissions. The subject is interesting and useful. However, there are several issues that need to be improved before it can be accepted. My detailed comments are listed below:

1. Ln 73-77 recent references for modelling of nitrification inhibitor should be included. For example, Y Li et al., 2020. Modelling nitrification inhibitor effects on emissions of nitrous oxide (N2O) in the UK, Science of The Total Environment, 709: 136156.

This paper, which had not been published when I submitted the manuscript last year, is now cited. I also contrast this model with ours in Sec. 6.5 which has been added to the manuscript.

2. Original model seems too long although most of them are putted in Supplementary materials. This distracts from the modified parts and novelties. It would be better if this paper can focus more on the modified parts of nitrification inhibitor. I would like to use a subsection to describe briefly the original model, such as oxidation reduction reaction. On the other hand, Section 2.9 should include more details, such as some equations related to the modification of nitrification inhibitor.

I have reworded sec. 2.1 to clarify the relationship between the description of earlier model components in sec. 2.2 to 2.8, and nitrification inhibition in sec. 2.9. However because readers' understanding sec. 2.9 requires their understanding of sec. 2.2 to 2.8, I am reluctant to abbreviate them, as I frequently refer to these sections to explain model behavior in the Discussion. In fact, Sec. 2.9 includes all equations by which NI activity is modelled in this paper. I have removed Sec. 2.10 and 2.11, and all later references to them, to shorten the manuscript.

3. For the site description, it is better to add a figure to show the location of specific fields.

There was only 1 set of experimental plots located in only 1 field in this study. Further details about plot topography and size have been added to Sec. 3.1 with further details in an earlier paper by Lin et al. (2018)

4. Ln240, the Arrhenius equation of fTs could be given.

I now cite the Arrhenius equation in sec. 2.9 as [A6] in S1 of the Supplementary material in which all parameters are given.

5. It is unclear what Fall and Spring in Fig. 2 are since Fig. 2 (a)-(d) were in 2014-2016.

I have added seasonal indicators to Fig. 2.

6. It may not be sufficient to examine the sensitivity of one parameter, KiNH4 (Table 9) because other parameters should be important, such as RI, K_CO2 and temperature coefficients in fTs.

I examine the sensitivity to two parameters, It=0 and KiNH4 which could not be estimated from experimental studies. The other 2 parameters, RI and Fts could at least be estimated from other studies, although I now discuss issues concerning this estimation in Sec. 6.5 which had been added to the paper.

7. What is ftl in Eq. (3)?

This has been corrected to f_{Tsl} as in Eq. 1.

8. Other factors, such as soil moisture and pH, can also affect N2O emission with the nitrification inhibitor. The limitations should be discussed due to the neglection of these factors.

I have added a note to this effect in Sec. 6.4, but insufficient data are available for model parameterization.

Anonymous Referee #3

Nitrification inhibitors (NI) have attracted much interest recently because retarding nitrification by NI can reduce the emission of N2O from farmland, thus reducing the climate forcing of food production. However, it is difficult to simulate effects of nitrification inhibitors on N2O emission from agriculture due to complex interaction among NI, nutrients, soils and weather. This paper modified Ecosystem model to incorporate NI processes and applied it to evaluate effects of NI on N2O emissions. Thus, the topic of the paper is highly relevant. However, it may require some changes before acceptance for publication. Below is a list of major and minor comments.

Major comments

1. Many of the described method in this study are already stated in their previous works. Some of them have included from their previously published works.

I have retained sec. 2.2 to 2.8 because readers' understanding sec. 2.9 on NI requires their understanding of sec. 2.2 to 2.8, and I frequently refer to these sections to explain model behavior in the Discussion. I have removed Sec. 2.10 and 2.11, and all later references to them, to shorten the manuscript.

2. In Section 3.1, more details are needed; for example, describe the vegetation, in terms of species, snow depth, drainage patterns of the fields, slope, ... This information will help for repeatability of this study. Also, this information can be used in a larger study for globalizing the model capability addressed in this study.

I have added a few further details about the experimental site in Sec. 3.1, noting that this experiment was already described in an earlier publication (Lin et al., 2018).

3. In Section 4, it is unclear what site boundaries were modelled. Ecosystem could be a 3D model for water and nutrient transports in S4. Did the authors simulate the 3Dfluxes in soils in this study? More details should be provided for the site topology and slopes for a 3D simulation if yes.

Field plots were simulated as 1D soil profiles with a subsurface water table at 1.2 m as now described in Sec. 4.1.

4. In Section 5, though the paper stressed effects of snowmelt and freeze-thaw on NI and N2O emissions, no results were reported on the freeze-thaw processes, such as snowpack depths, and snowmelt water pools. For example, in Section 5.2.1, oxygen transfer and uptake are explained using snowmelt and drainage of meltwater. However, snowpack was not provided in both measurement and simulations. In Lines 439-441, the smaller rises and subsequent declines in N2O in Fig. 5 were attributed to effects of information of thawing and refreezing. However, Fig. 5 does not provide information of snow depth and freeze-thaw.

I have added further information in Sec. 5.2.1 about how snowmelt and freezing-thawing affect N2O fluxes modelled in ecosys. These effects are further described in Grant and Pattey (1999) as now cited in Sec. 5.2.1. To some extent freezing and thawing can be inferred from temperatures plotted in Figs 4

through 7. I have not added any further graphics about snowmelt and soil thawing because the focus of this paper is on NI effects on N2O emissions rather than the emissions themselves, and the paper is already rather long.

Minor comments

5. Lines 49-51, give references.

Done

6. Lines 74-77, a testing of modelled NI effects on N2O emissions has been performed in Science of The Total Environment recently.

This paper, which had not been published when I submitted the manuscript last year, is now cited. I also contrast this model with ours in Sec. 6.5 which has been added to the manuscript.

7. In Conclusions, it is better to include quantitative results of NI effects.

I have added a range of N2O emission reductions modelled with NI

Formatted: Left

Modelling Nitrification Inhibitor Effects on N_2O Emissions after Fall and Spring-Applied Slurry by Reducing Nitrifier NH_4^+ Oxidation Rate

Grant, Robert.F.[1*], Lin, Sisi[1] and Hernandez-Ramirez, Guillermo[1]

[1] ***Department of Renewable Resources, University of Alberta, Edmonton, AB, Canada T6G 2E3***

ABSTRACT

Reductions in N_2O emissions from nitrification inhibitors (NI) are substantial, but remain uncertain because measurements of N_2O emissions are highly variable and discontinuous. Mathematical modelling may offer an opportunity to estimate these reductions if the processes causing variability in N_2O emissions can be accurately simulated. In this study, the effect of NI was simulated with a simple, time-dependent algorithm to slow NH_4^+ oxidation in the ecosystem model *ecosys*. Slower nitrification modelled with NI caused increases in soil NH_4^+ concentrations and reductions in soil NO_3^- concentrations and in N_2O fluxes that were consistent with those measured following fall and spring applications of slurry over two years from 2014 to 2016. The model was then used to estimate direct and indirect effects of NI on seasonal and annual emissions. After spring slurry applications, NI reduced N_2O emissions modelled and measured during the drier spring of 2015 (35% and 45%) less than during the wetter spring of 2016 (53% and 72%). After fall slurry applications, NI reduced modelled N_2O emissions by 58% and 56% during late fall in 2014 and 2015, and by 8% and 33% during subsequent spring thaw in 2015 and 2016. Modelled reductions were consistent with those from meta-analyses of other NI studies. Simulated NI activity declined over time, so that reductions in N_2O emissions modelled with NI at an annual time scale were relatively smaller than those during emission events. These

reductions were accompanied by increases in NH_3 emissions and reductions in NO_3^- losses with NI that caused changes in indirect N_2O emissions. With further parameter evaluation, the addition of this algorithm for NI to *ecosys* may allow emission factors for different NI products to be derived from annual N_2O emissions modelled under diverse site, soil, land use and weather.

1. INTRODUCTION

Nitrification inhibitors (NI) have frequently been found to reduce N_2O emissions from fertilizer and slurry applications in agricultural fields. In a meta-analysis of field experiments conducted to 2008, Akiyama et al. (2010) found average reductions of 38 ± 6% in N_2O emissions from NI with some variation attributed to land use type and emission rates. Similar average reductions of 35 - 40% were reported in more recent meta-analyses by Ruser and Schulz (2015), Gilsanz et al. (2016) and Gao and Bian (2017). However the magnitudes of these reductions are uncertain because they vary with rate and timing of fertilizer or slurry application, with land use and ecosystem type (Akiyama et al., 2010) and with application method (Zhu et al., 2016). These magnitudes are also uncertain because measurements of the N_2O emissions on which they are based are highly variable temporally and spatially, and difficult to sustain over the annual time periods needed to estimate NI reductions.

The effects of NI on N_2O emissions are attributed to inhibition of ammonia monooxygenase which slows the oxidation of NH_4^+ to NO_2^- during nitrification (Subbarao et al., 2006), and hence slows the reduction of NO_2^- to N_2O during nitrifier denitrification. The consequent slowing of NO_2^- oxidation to NO_3^- would also slow the reduction of NO_3^- to N_2O during denitrification. The effectiveness of NI has been found to decline over time due to mineralization, adsorption and volatilization, depending on NI formulation. The rate of this decline varies among NI products and soil types, and increases with soil temperature (Guardia et al., 2018).

The great majority of the studies included in meta-analyses of NI effects on N_2O emissions were conducted following fertilizer or slurry application on warm soils in spring or summer (e.g. Akiyama et al., 2010). The effectiveness of NIs with fall applications of fertilizer

or slurry on cold soils has thus far received very limited attention (Ruser and Schulz, 2015), although in cold climates N_2O emissions during the spring thaw following fall applications may exceed those during later spring and summer following spring applications (Lin et al., 2018). Emissions during spring thaw were attributed by Wagner-Riddle and Thurtell (1998) to soil NO_3–N concentrations exceeding 20 mg kg^{-1} generated by fall-applied slurry that contributed to total N_2O emissions exceeding 0.2 g N m^{-2} measured between January and April of the following year. Large N_2O emissions measured in late winter were attributed by Dungan et al. (2017) to labile N not used by soil microorganisms during the previous fall and winter that was actively metabolized when the soils began to warm in early March. Interannual differences in spring thaw emission events after fall slurry applications were related by Kariyapperuma et al. (2012) to those in total soil mineral N content in the upper 15 cm of the soil profile during spring thaw. The effects of NI on N_2O emissions during spring thaw will therefore depend on the persistence with which NI reduces nitrification in cold soils during fall and winter, and thereby alters mineral N concentrations during the following spring.

Reductions in N_2O emissions directly caused by slower nitrification with NI may be partially offset by increases in indirect N_2O emissions from increasing NH_3 emissions caused by greater soil NH_4^+ concentrations (Lam et al., 2017, Qiao et al., 2015). NI may also decrease indirect N_2O emissions by reducing NO_3^- concentrations and hence leaching. Both direct and indirect effects of NI on N_2O emissions must be considered when estimating effects of NI on total N_2O emissions.

IPCC Tier 3 methodology for estimating N_2O emissions under diverse climates, soils, fertilizers and land uses includes the use of comprehensive, process-based mathematical models of terrestrial C, N, water and energy cycling (IPCC, 2019). Although NI effects on nitrification have been added to some existing process models (Cui et al., 2014; Del Grosso et al., 2009, Li et al., 2020), testing of modelled NI effects on N_2O emissions against measurements remains limited to brief periods following soil N amendments (e.g. Giltrap et al., 2011). The mathematical model *ecosys* explicitly represents the key processes in nitrification (Grant, 1994), denitrification (Grant, 1991) and associated N_2O emissions (Grant, 1995), and has been tested against measurements of N_2O emissions using micrometeorological methods, and manual and automated chambers (Grant and Pattey, 1999, 2008; Grant et al., 2006, 2016; Metivier et al.,

2009). In this study, we propose that applying a time-dependent reduction of NH_4^+ oxidation rates during nitrification will enable *ecosys* to simulate the time course of reductions in N_2O emissions with NI measured after fall and spring applications of dairy slurry in a field experiment. The model is then used to estimate the direct and indirect effects of NI on annual N_2O emissions with fall and spring slurry applications as required for IPCC Tier 3 methodology, and how these effects would change with alternative tillage practices and timings of slurry application.

2. MODEL DEVELOPMENT

2.1.General Overview

The hypotheses for oxidation-reduction reactions involving N_2O, and the aqueous and gaseous transport of their substrates and products, are represented in Fig. 1 and described in further detail below. ~~References to equations and definitions listed in Supplements S1, S3, S4, S5 and S8 of the Supporting Information (Table 1) are provided for those interested in model methodology, but are not needed for a general understanding of model behaviour.~~ These hypotheses function within a comprehensive model of soil C, N and P transformations, which is coupled to ~~one~~ models of soil water, heat and solute transport in surface litter and soil layers~~,~~. ~~which~~ These models ~~are in turn components of the~~function within the comprehensive ecosystem model *ecosys*. Key transformations that drive N_2O emissions are described in Sections 2.2 to 2.8 below, and modifications of these transformations to simulate nitrification inhibition are described in Section 2.9. References to equations and definitions ~~listed~~ in Sections 2.2 to 2.8 and given in Supplements S1, S3, S4, S5 and S8 of the Supporting Information (Table 1) are provided for those interested in model methodology, but are not needed for a general understanding of model behaviour.

Formatted: Subscript

2.2.Mineralization and Immobilization of Ammonium by Microbial Functional Types

Heterotrophic microbial functional types (MFTs) *m* (obligately aerobic bacteria, obligately aerobic fungi, facultatively anaerobic denitrifiers, anaerobic fermenters, acetotrophic

methanogens, and obligately aerobic and anaerobic non-symbiotic diazotrophs) are associated with each organic substrate *i* (*i* = manure, coarse woody plant residue, fine non-woody plant residue, particulate organic matter, or humus). Autotrophic MFTs *n* (aerobic NH_4^+ and NO_2^- oxidizers, aerobic methanotrophs and hydrogenotrophic methanogens) are associated with inorganic substrates. These MFTs grow [A25] with energy generated from oxidation of dissolved organic C (DOC) by heterotrophs [H2, H10], of acetate by acetotrophic methanogens, of mineral N (NH_4^+ and NO_2^-) [H11, H15] by nitrifiers, of CH_4 by methanotrophs [G7], or of H_2 by hydrogenotrophic methanogens [G12], coupled with reduction of e^- acceptors O_2 [H4, G22], acetate [G8], NO_x [H7 – H9], and CO_2 [G13]. These MFTs decay according to first-order rate constants [A23] with internal recycling of resources (C, N, P) from structural to nonstructural components *j* (*j* = labile, recalcitrant, nonstructural) varying with nonstructural C:N:P ratios [A24], the decay products of which form humus C, N and P [A35, A36]. Each MFT seeks to maintain a set nonstructural C:N:P ratio by mineralizing NH_4^+ and H_2PO4^- [H1a] from, or by immobilizing NH_4^+, NO_3^- and H_2PO4^- [H1b, H1c] into, its nonstructural N and P components. These transformations control the exchange of N and P between organic and inorganic states, and of O_2 between aqueous and gaseous states, and hence affect the availability of substrates and e^- acceptors for nitrification and denitrification.

2.3. Oxidation of DOC and Reduction of Oxygen by Heterotrophs

N_2O is generated when demand for e^- acceptors from oxidation by aerobic heterotrophs and autotrophs (Sec. 2.2) exceeds supply from O_2, requiring explicit modelling of O_2 transport and uptake, and consequent O_2 constraints to oxidation-reduction reactions ~~(Sec. 2.11 below)~~ (Fig. 1). Constraints on heterotrophic oxidation of DOC imposed by O_2 uptake are solved in four steps:

1) DOC oxidation by heterotrophs under non-limiting O_2 is calculated from specific oxidation rates multiplied by active biomasses and an Arrhenius function of T_s~~,~~ [A6] used for all microbial transformations, constrained by DOC concentration [H2],
2) O_2 reduction to H_2O under non-limiting O_2 (O_2 demand) by aerobic heterotrophs is calculated from step 1 using a set respiratory quotient [H3],
3) O_2 reduction to H_2O under ambient O_2 is calculated from radial O_2 diffusion through water films with thicknesses determined by soil water potential [H4a] coupled with active uptake at

heterotroph surfaces driven by step 2 [H4b]. Diffusion and uptake are sustained by O_2 transfer through soil aqueous and gaseous phases controlled by soil water- and air-filled porosity governed by freezing, thawing and transfer of soil water [D14 – D20]. O_2 diffusion and active uptake are calculated for each heterotrophic population associated with each organic substrate, allowing [H4] to calculate lower O_2 concentrations at microbial surfaces (O_{2m}) associated with more biologically active substrates (e.g. manure, litter). Localized zones of low O_2 concentration (hotspots) are thereby simulated when O_2 uptake by any aerobic MFT is constrained by O_2 diffusion to that functional type. O_2 uptake by each heterotrophic MFT is affected by competition for O_2 uptake with other heterotrophs, nitrifiers, roots and mycorrhizae, calculated from its biological O_2 demand relative to those of other aerobic functional types.

4) DOC oxidation to CO_2 under ambient O_2 is calculated from steps 2 and 3 [H5]. The energy yield of DOC oxidation with O_2 reduction drives the uptake of additional DOC for construction of microbial biomass $M_{i,h}$ according to construction energy costs of each heterotrophic functional type [A21]. Energy costs of denitrifiers are slightly larger than those of obligately aerobic heterotrophs, placing denitrifiers at a small competitive disadvantage for growth and hence DOC oxidation under non-limiting O_2.

2.4. Oxidation of DOC and Reduction of Nitrate, Nitrite and Nitrous Oxide by Denitrifiers

N_2O may be both product and substrate of NO_x reduction coupled with DOC oxidation by denitrifiers. Constraints imposed by NO_3^- availability on denitrifier DOC oxidation are solved in five steps:

1) NO_3^- reduction to NO_2^- by heterotrophic denitrifiers under non-limiting NO_3^- is calculated from demand for e^- acceptors by denitrifiers for DOC oxidation to CO_2, but not met from O_2 reduction to H_2O because of diffusion limitations to O_2 supply (Sec. 2.3 step 3). This unmet demand is transferred to NO_3^- [H6],
2) NO_3^- reduction to NO_2^- under ambient NO_3^- is calculated from step 1, accounting for relative concentrations and affinities of NO_3^- and NO_2^- [H7],

3) NO_2^- reduction to N_2O under ambient NO_2^- is calculated from demand for e^- acceptors not met by NO_3^- reduction in step 2, accounting for relative concentrations and affinities of NO_2^- and N_2O. This unmet demand is transferred to NO_2^- [H8].
4) N_2O reduction to N_2 under ambient N_2O is calculated from demand for e^- acceptors not met by NO_2^- reduction in step 3, and hence transferred to N_2O [H9].
5) additional energy yield from DOC oxidation to CO_2 enabled by NO_x reduction in steps 2, 3 and 4 is added to that enabled by O_2 reduction from [H5], which drives additional DOC uptake for construction of $M_{i,n}$. This additional uptake offsets the disadvantage incurred by the larger construction energy costs of denitrifiers (Sec. 2.3 step 4).

2.5. Oxidation of Ammonium and Reduction of Oxygen by Nitrifiers

N_2O may also be generated by reduction of NO_2^- coupled with oxidation of NH_4^+ by autotrophic nitrifiers. Constraints on nitrifier oxidation of NH_4^+ imposed by O_2 uptake are solved in four steps:

1) Oxidation of NH_4^+ (in dynamic equilibrium with NH_3 [E24]) under non-limiting O_2 is calculated from a specific oxidation rate multiplied by active biomass and an Arrhenius function of T_s, and constrained by NH_4^+ and CO_2 concentrations [H11],
2) O_2 reduction to H_2O under non-limiting O_2 (O_2 demand) is calculated from step 1 using set respiratory quotients [H12],
3) O_2 reduction to H_2O under ambient O_2 is calculated from radial O_2 diffusion through water films of thickness determined by soil water potential [H13a] coupled with active uptake at nitrifier surfaces driven by step 2 [H13b]. O_2 uptake by nitrifiers is affected by competition for O_2 uptake with heterotrophic DOC oxidizers, roots and mycorrhizae, calculated from its biological O_2 demand relative to those of other aerobic functional types.
4) NH_4^+ oxidation to NO_2- under ambient O_2 is calculated from steps 2 and 3 [H14]. The energy yield of NH_4^+ oxidation drives the fixation of CO_2 for construction of microbial biomass $M_{i,n}$ according to nitrifier construction energy costs.

2.6.Oxidation of Nitrite and Reduction of Oxygen by Nitrifiers

Constraints on nitrifier oxidation of NO_2^- to NO_3^- imposed by O_2 uptake [H15 - H18] are solved in the same way as are those of NH_4^+ to NO_2^- [H11 - H14]. The energy yield of NO_2^-

451 oxidation drives the fixation of CO_2 for construction of microbial biomass $M_{i,o}$ according to
452 nitrifier construction energy costs.
453

454 **2.7. Oxidation of Ammonium and Reduction of Nitrite by Nitrifiers**

455 In both nitrifier and denitrifier processes, N_2O is generated from reduction of NO_2^-, the
456 availability of which is controlled by NO_2^- oxidation (Sec. 2.6). Under low O_2 concentrations
457 NO_2^- oxidation is suppressed [H18], favoring NO_2^- reduction. Constraints on nitrifier oxidation
458 of NH_4^+ imposed by NO_2^- availability are solved in three steps:
459 1) NO_2^- reduction to N_2O under non-limiting NO_2^- is calculated from e^- acceptors demanded by
460 NH_4^+ oxidation to NO_2^- but not met by O_2 for reduction to H_2O because of diffusion
461 limitations to O_2 supply, and hence transferred to NO_2^- [H19],
462 2) NO_2^- reduction to N_2O under ambient NO_2^- and CO_2 is calculated from step 1 [H20],
463 competing for NO_2^- with denitrifiers [H8] and nitrifiers [H18],
464 3) energy yield from additional NH_4^+ oxidation to NO_2^- enabled by NO_2^- reduction in step 2
465 [H21] is added to that enabled by O_2 reduction from Sec. 2.5 step 4 [H14] which drives the
466 fixation of additional CO_2 for construction of $M_{i,n}$.
467

468 **2.8. Uptake of Ammonium and Reduction of Oxygen by Roots and Mycorrhizae**

469 NH_4^+ oxidation and O_2 reduction by nitrifiers compete for substrates with NH_4^+ uptake
470 and O_2 reduction by other MFTs, and by roots and mycorrhizae.
471 1) NH_4^+ uptake by roots and mycorrhizae under non-limiting O_2 is calculated from mass flow
472 and radial diffusion between adjacent roots and mycorrhizae [C23a] coupled with active
473 uptake at root and mycorrhizal surfaces [C23b]. Active uptake is subject to product inhibition
474 by root nonstructural N:C ratios [C23g] where nonstructural N is the active uptake product,
475 and nonstructural C is the CO_2 fixation product transferred to roots and mycorrhizae from the
476 canopy.
477 2) O_2 reduction to H_2O under non-limiting O_2 is calculated from O_2 demands for NH_4^+ uptake in
478 step 1, and for oxidation of root and mycorrhizal nonstructural C for root maintenance and
479 growth using a set respiratory quotient [C14e],

3) O_2 reduction to H_2O under ambient O_2 is calculated from mass flow and radial diffusion between adjacent roots and mycorrhizae [C14d] coupled with active uptake at root and mycorrhizal surfaces driven by step 2 [C14c]. O_2 uptake by roots and mycorrhizae is also affected by competition with O_2 uptake by heterotrophic DOC oxidizers, and autotrophic nitrifiers, calculated from their biological O_2 demands relative to those of other populations.
4) oxidation of root and mycorrhizal nonstructural C to CO_2 under ambient O_2 is calculated from steps 2 and 3 [C14b],
5) NH_4^+ uptake by roots and mycorrhizae under ambient O_2 is calculated from steps 1, 2, 3 and 4 [C23b].

2.9. Nitrification Inhibition

For this study, NIs were assumed to reduce specific rates of NH_4^+ oxidation by nitrifiers in Sec. 2.5 step 1, thereby simulating inhibition of ammonia monooxygenase (Subbarao et al., 2006). This reduction was represented by a time-dependent scalar I:

$$I_{t_l} = I_{t\text{-}1_l} - I_{t\text{-}1_l} * R_I * f_{Ts_l} \quad [1]$$

where t is the current time step (h), t-1 is the previous time step (h), I is the inhibition (initialized to 1.0 at t = 0 at the time of application), R_I is the rate constant for decline of I representing NI degradation (set to 2.0 x 10^{-4} h^{-1} for more persistent NIs such as DMPP and to 1.0 x 10^{-3} h^{-1} for less persistent NIs such as nitrapyrin (Ruser and Schulz, 2015)), f_{Ts} is an Arrhenius function of soil temperature (T_s) used to simulate T_s effects on microbial activity ([A6] in Sec. 2.3 step 1), and l is the soil layer in which NI is present. The values of R_I and f_{Ts} for DMPP were selected to give time and temperature dependencies of DMPP activity following application inferred from incubation studies by Guardia et al. (2018). Model results for NI presented below are those using the smaller R_I for DMPP unless stated as those using the larger R_I for nitrapyrin.

Specific rates of NH_4^+ oxidation (Sec. 2.5 step 1) with NI was calculated as:

$$X'_{NH4t_l} = X''_{NH4_l} * (1.0 - I_{t_l} / (1.0 + [NH_4^+]_l / K_{iNH4})) \quad [2]$$

where X'_{NH4} and X''_{NH4} are specific NH_4^+ oxidation rates with and without NI (g N g nitrifier C^{-1} h^{-1}), $[NH_4^+]$ is the aqueous NH_4^+ concentration (g N m^{-3} in dynamic equilibrium with $[NH_3]$), and K_{iNH4} is an inhibition constant set at 7000 g N m^{-3} to reduce inhibition at very large $[NH_4^+]$ as suggested in Janke et al. (2019). These rates were used to calculate nitrification rates [H11]:

$$X_{NH4t_l} = X'_{NH4t_l} M_{n_l} f_{Ts_l} f_{t_l} \{[NH_4^+]_l / ([NH_4^+]_l + K_{NH4})\} \{[CO_2s]_l / ([CO_2s]_l + K_{CO2})\} \quad [3]$$

where X_{NH4t} is the nitrification rate (g N m^{-2} h^{-1}), M_n is the nitrifier biomass (g C m^{-2}) and K_{NH4} and K_{CO2} are half-saturation constants for aqueous NH_4^+ and CO_2 (g N and C m^{-3}). NI in Eq. 1 slows X'_{NH4t} in Eq. 2 and thereby X_{NH4t} in Eq. 3, and hence slows NO_2^- production from nitrification (Sec. 2.5 step 4), and thereby N_2O production from nitrification (Sec. 2.7 step 2) and denitrification (Sec. 2.4 step 3). By slowing X_{NH4t} in Eq. 3, NI also reduces nitrification energy yield and hence M_n growth, biomass [A25] and O_2 uptake [H13], thereby further reducing N_2O production.

~~**2.10. Cation Exchange and Ion Pairing of Ammonium**~~

~~Availability of NH_4^+ to nitrifiers is also controlled by NH_4^+ adsorption. A Gapon selectivity coefficient is used to solve cation exchange of NH_4^+ vs. Ca^{2+} [E10] as affected by other cations [E11] – [E15] and CEC [E16]. A solubility product is used to equilibrate soluble NH_4^+ and NH_3 [E24] as affected by pH [E25] and other solutes [E26 – E57]. Equilibrium NH_4^+ concentrations drive NH_4^+ oxidation (Sec. 2.5 step 1) and NH_3 volatilization (Sec. 2.11 below).~~

~~**2.11. Soil Transport and Surface – Atmosphere Exchange of Aqueous and Gaseous Substrates and Products**~~

~~O_2 uptake and N_2O emissions in Sec. 2.3 to 2.8 above are governed by aqueous and gaseous transport processes in vertical and lateral directions:~~

~~1) Exchanges of all modelled gases γ (γ = O_2, CO_2, CH_4, N_2, N_2O, NH_3 and H_2) between aqueous and gaseous states within each soil layer are driven by disequilibrium between aqueous and gaseous concentrations according to a T_s dependent solubility coefficient,~~

~~constrained by an interphase transfer coefficient based on air-water interfacial area that depends on air-filled porosity (θ_g) [D14 – D15] (Fig. 1).~~

~~2) These gases undergo vertical and lateral convective-dispersive transport through soil in gaseous [D16] and aqueous [D19] states driven by soil water flux and by gas concentration gradients. Dispersive transport is controlled by gaseous diffusion [D17] and aqueous dispersion [D20] coefficients calculated from θ_g and water-filled porosity (θ_w). Both θ_g and θ_w are affected by ice-filled porosity (θ_i) from freezing and thawing driven by soil heat fluxes [D13].~~

~~3) Vertical exchanges of all gases between the atmosphere and both gaseous and aqueous states at the soil surface are driven by atmosphere – surface gas concentration differences and by boundary layer conductance above the soil surface, calculated from wind speed and from vegetation density and surface litter [D15]. These exchanges give modelled surface fluxes used in tests against surface fluxes measured in field experiments.~~

~~4) All solutes can be lost/gained by lateral surface runoff/runon, modelled from Manning's equation [D1a] with surface water depth [D2] calculated from surface water balance [D4] using kinematic wave theory, and by lateral subsurface discharge/recharge modelled from convective exchange through subsurface boundaries with an external water table.~~

3. FIELD EXPERIMENT

3.1. Site Description and Experimental Design

An experiment was established on a Black Chernozem (Table 2) under barley (*Hordeum vulgare* L.) silage from 2014 to 2016 on a level site at the South Campus Farm in Edmonton, AB, Canada (53°29'30″N, 113°31'53″W~~),~~). The experimental design ~~using~~ was an incomplete split-plot ~~design~~ (main plot: fall vs. spring application of dairy slurry; split plot: control vs. NI treatments) on plots 2.4 m in width and 6.1 m in length with three replicates. ~~(Lin et al., 2018)~~. The NI products ENTEC (Eurochem Agro, Mannheim, Germany) and eNtrench Nitrogen Stabilizer (Dow Chemical Company, Dow AgroSciences, Calgary, AB, Canada) were mixed with the slurry immediately before application to provide 0.4 kg ha^{-1} active ingredient with slurry injection of 56.17 m^3 ha^{-1} at 12.7 to 15.2 cm (average 14 cm) depth and 28 cm spacing. Measured concentrations of NH_4^+ and of organic N and C in each slurry application were used to

Formatted: Font: Italic

Formatted: Font: Italic

calculate rates of NH_4^+, organic N and organic C amendments (Table 3). Soil NH_4^+ concentrations were measured from 0 to 10 cm every 2 – 3 weeks between spring thaw and autumn freezing in 2014, 2015 and 2016. Further details of this field experiment are given in Lin et al., (2018).

Weather data (radiation, air temperature (T_a), humidity, windspeed and precipitation) were recorded hourly from 2012 through 2016 at the South Campus Farm. During the first experimental year (16 Sep. 2014 to 15 Sep. 2015) T_a remained 1 – 2 °C higher than historical (1981 – 2010) averages (Lin et al., 2018) (Table 4). Precipitation was slightly higher than historical averages during autumn and winter, but was about one-half those during spring and summer. During the second experimental year (16 Sep. 2015 to 15 Sep. 2016), T_a was higher than that of the first year during winter and early spring, and similar during late spring and summer. However precipitation during the second year was lower from autumn to early spring and much higher during late spring and summer.

3.2. N_2O Flux Measurements

N_2O fluxes were measured at 3-h intervals from as soon as ~~possible~~ field conditions allowed after spring thaw to late summer during both experimental years with automated chambers (height 26 cm, area 0.216 m^2) connected by 0.5 cm i.d. tubes to a FTIR gas analyzer (GASMET model CX4025, Temet Instruments, Finland) through which air flow was maintained at 5.1 L min^{-1}. During each 20 minute measurement period, the chambers remained open for the first 5 minutes to restore ambient N_2O concentrations in the gas analyzer, after which chambers were closed and N_2O concentrations were measured at 10 Hz and averages recorded at 1 minute intervals. Concentrations during the first minute after closure were discarded and those during the following 14 minutes were used to calculate fluxes using linear regression with an acceptance criterion of $R^2 \geq 0.85$. Based on the analytical precision of the gas analyzer, the N_2O flux detection limit was determined to be +/- 0.03 mg N m^{-2} h^{-1}.

N_2O emissions were also measured once or twice per week from spring thaw to autumn freezing during both experimental years with manually operated chambers as described in Lin et al. (2018). The time required for installation of the automated chambers after snowmelt limited

their ability to measure N_2O emissions during spring thaw, so that measurements from the manually operated chambers were used to evaluate emissions during these periods.

4. MODEL EXPERIMENT

4.1. Model Spinup

To simulate site conditions prior to the experiment, *ecosys* was initialized with the properties of the Black Chernozem, simulated as a one-dimensional profile (Table 2) with surface water runoff and subsurface water exchange with a water table at 1.2 m depth. ~~and~~ The model was run from model dates 1 Jan. 1992 to 31 Dec. 2013 under a repeating 5-year sequence of weather data (radiation, air temperature (T_a), humidity, windspeed and precipitation recorded hourly from 2012 through 2016 at the South Campus Farm. The soil was During each year of the spinup run, barley was planted, fertilized and harvested as silage to reproduce land use practices reported from the field site.

4.2. Model Runs

The spinup run was extended from 1 Jan. 2014 to 31 Dec. 2016 under weather data recorded from 2014 to 2016 with the land use schedules and practices from the field site (Table 3). Each modelled slurry application was added to the soil layer the depth of which corresponded to that of slurry injection in the field experiment (14 cm). Modelled applications were accompanied by addition of water corresponding to the volume and depth of the application (5.6 mm from 56.17 m^3 ha^{-1} at 14 cm in Sec. 3.1), and by tillage using a coefficient for surface litter incorporation and soil mixing of 0.2 to the depth of application (14 cm), based on field observations. A control run was also conducted in which no slurry applications were modelled. For all silage harvests, cutting height and harvest efficiency were set to 0.15 m and 0.9, so that 0.9 of all plant material above 0.15 m was removed as yield. Concentrations of NH_4^+ and NO_3^-, and N_2O emissions modelled during key emission events, were compared with measured values (Sec. 3.1 and 3.2), and modelled emissions were then aggregated into seasonal and annual values.

There is some flexibility in the timing of fall slurry application between crop harvest in late summer and soil freezing in early November. To examine how timing of fall slurry application

633 would affect subsequent N_2O emissions with and without NI, fall slurry application dates were
634 advanced or delayed by 2 weeks from those in Table 3, and effects on spring and annual N_2O
635 emissions were evaluated. To examine how increased tillage during slurry application would
636 affect subsequent N_2O emissions with and without NI, coefficients for surface litter
637 incorporation and soil mixing to the depth of slurry application were raised from 0.2 to 0.5 and
638 0.8 for fall and spring applications.
639

640 ## 5. RESULTS

641

642 ### 5.1. NI and Soil NH_4^+ and NO_3^- Concentrations

643 #### 5.1.1. Fall Slurry Applications

644 In the model, NI slowed NH_4^+ oxidation (Sec. 2.9, Eq. 3) so that declines in NH_4^+
645 concentrations modelled and measured after fall and spring slurry applications with NI were
646 slower than those without NI (Fig. 2a), particularly during winter when declines in inhibition
647 were slowed by low T_s (Sec. 2.9, Eq. 1) following the onset of soil freezing modelled at the depth
648 of slurry injection (DOY 313 in 2014 and DOY 318 in 2015 in Fig. 2a). Overwinter declines in
649 NH_4^+ concentrations were slower during the winter of 2015/2016 with lower T_s modelled under
650 less winter precipitation and hence shallower snowpack (Table 4). These slower declines caused
651 larger NH_4^+ concentrations to be modelled during the following spring, consistent with
652 measurements (Fig. 2a). The slower declines in NH_4^+ concentrations modelled with NI caused
653 slower rises in NO_3^- concentrations following fall slurry applications (Fig. 2c). However slower
654 rises with NI were not always apparent in the measured NO_3^- concentrations.

655

656 #### 5.1.2. Spring Slurry Applications

657 Declines in NH_4^+ concentrations modelled after slurry applications with NI in spring 2015
658 and 2016 were also slower than after those without NI (Fig. 2b), consistent with higher NH_4^+
659 concentrations measured after spring application with DMPP in both years (Fig. 2b). These
660 slower declines caused slower rises in NO_3^- concentrations to be modelled following spring
661 slurry applications with NI (Fig. 2d).

662

5.2. NI and Soil Gas Concentrations

5.2.1. Fall Slurry Applications

In the model, soil ice impeded drainage during spring snowmelt and soil thaw, ~~raised~~ raising θ_w and ~~lowered~~ lowering θ_g, and thereby slowing gas transfers in gaseous phases and gas exchanges between gaseous and aqueous phases ~~(Sec. 2.11 step 1, 2)~~ (Sec. 2.3 step 3; Fig. 1). Freeze-thaw effects on N_2O emissions modelled during early spring are further described in Grant and Pattey (1999). Slower O_2 transfers relative to O_2 uptake (Sec. 2.3, 2.5 and 2.6) forced reductions in aqueous O_2 concentrations (O_{2s}) to be modelled during early spring in 2015 (Fig. 3a,b) and 2016 (Fig. 3c,d) following fall slurry applications in 2014 and 2015. Declines in aqueous O_2 (O_{2s}) were later but more rapid in 2015 than in 2016, following greater winter precipitation and hence greater snowmelt in 2014/2015 (Table 4). Earlier and more persistent declines in O_{2s} were modelled in 2016 because greater θ_l modelled with less thermal insulation under a shallower snowpack ~~(Sec. 2.11 step 2)~~ reduced or eliminated θ_g during much of the winter. Drainage of meltwater after snowmelt eventually lowered θ_w and raised θ_g, allowing O_{2s} to return to atmospheric equivalent concentrations.

Formatted: Subscript

Formatted: Subscript

Declines in O_{2s} in slurry-amended treatments drove increases in aqueous N_2O concentrations (N_2O_s) (Fig. 3b,d) during winter and early spring (Sec. 2.7, step 1). These rises were similar with and without NI, in spite of higher NH_4^+ concentrations without NI (Fig. 2a). Rises in θ_g following spring drainage allowed volatilization of N_2O from aqueous to gaseous phases ~~(Sec. 2.11 step 1)~~, reducing N_2O_s and driving N_2O emissions modelled during spring thaw.

5.2.2. Spring Slurry Applications

Declines in O_{2s} modelled after spring slurry application were small during the drier spring of 2015 (Table 4) (Fig. 3e), but were greater with lower θ_g during the wetter spring of 2016 (Fig. 3g) ~~(Sec. 2.11)~~. During both years, these declines were more rapid with slurry than without, but less rapid with NI-amended slurry than with unamended slurry. Greater declines in O_{2s} modelled in 2016 vs. 2015 drove greater increases in N_2O_s (Sec. 2.7), particularly without NI, and hence greater emissions of N_2O ~~(Sec. 2.11)~~ during subsequent declines in N_2O_s.

5.3. NI and N_2O Fluxes

694 **5.3.1. Fall Slurry Applications**

695 Smaller rises and subsequent declines in N_2O_s modelled with NI than without (Fig. 3b) drove
696 smaller N_2O emission events modelled during spring thaw in 2015 (Fig. 4a) following slurry
697 application in fall 2014 (Fig. 4b). These events were driven by increases in θ_g during
698 midafternoon thawing of near-surface soil ~~(Sec. 2.11 step 1)~~, but were terminated by loss of θ_g
699 during nighttime refreezing. These events preceded the start of the automated chamber
700 measurements on DOY 102 and so could not be corroborated by them. However measurements
701 with manual chambers earlier in spring 2015 by Lin et al. (2018) indicated that N_2O emission
702 events occurred from DOY 85 to 100 that were similar in magnitude although not always in
703 timing with those modelled (Fig. 4b). These measured emissions were smaller with NI than
704 without, consistent with modelled emissions.
705
706 The smaller rises and subsequent declines in N_2O_s modelled with NI than without in the
707 winter of 2016 (Fig. 3d) drove smaller emission events during thawing and refreezing of near-
708 surface soil in spring 2016 (Fig. 5a) following slurry application in fall 2015 (Fig. 5b). These
709 modelled events preceded the start of automated chamber measurements on DOY 91, but earlier
710 measurements with manual chambers indicated N_2O emission events occurred from DOY 74 to
711 93. The smaller emission events modelled with NI were consistent with those measured using the
712 manual chambers, although some larger emissions measured with DMPP using the automated
713 chambers from DOY 91 to 102 were not modelled (Fig. 5b). In both years, emissions modelled
714 and measured without slurry remained very small, consistent with low N_2O_s (Fig. 3b,f).
715
716 **5.3.2. Spring Slurry Applications**

717 Modelled N_2O emissions closely followed measured values during a brief emission event
718 following slurry application in the drier spring of 2015 (Fig. 6a,b), driven by small rises and
719 declines in $N2O_s$ (Fig. 3f). The smaller rise and decline in N_2O_s modelled with NI than without
720 drove smaller N_2O emissions which declined more rapidly after application than did emissions
721 measured with DMPP (Fig. 6b).
722
723 Emissions modelled without NI in the wetter spring of 2016 were larger than those in the
724 drier spring of 2015 (Fig. 7a,b), driven by a larger rise and decline in N_2O_s with lower θ_g (Fig.

3h). These emissions were suppressed by low θ_g with soil wetting during heavy rainfall on DOY 141 – 143 shortly after slurry application (Fig. 7a,b), but resumed when θ_g rose with soil drainage thereafter (Fig. 7b). Emissions modelled without NI remained greater than those measured until DOY 150, after which modelled values declined with soil drying while measured value rose (Fig. 7b). Greater reductions in N_2O_s (Fig. 3h) and hence in N_2O emissions were modelled with NI after slurry application in the wetter spring of 2016 (Fig. 7b) than in the drier spring of 2015 (Fig. 6b). In both years, emissions modelled and measured without slurry remained very small, consistent with low N_2O_s (Fig. 3f,h).

5.4. NI Effects on Seasonal and Annual N_2O Emissions

5.4.1. Modelled vs. Measured N_2O Emissions after Spring Slurry Applications

Total N_2O emissions modelled without NI and with NI using R_I for DMPP or nitrapyrin (Sec. 2.9) were compared with those aggregated from automated chamber measurements over 30-day periods after spring slurry applications in 2015 and 2016 (Table 5). Total emissions modelled and measured without NI were greater during the wetter spring of 2016 than during the drier spring of 2015. Reductions in 30 d emissions modelled and measured with R_I for DMPP and nitrapyrin were greater during the wetter spring in 2016 (53% and 41%) than during the drier spring in 2015 (35% and 30%). These reductions were somewhat smaller than those measured with DMPP and nitrapyrin in 2016 (72% and 64%) and 2015 (45% and 36%). Emissions were not measured with automated chambers after fall slurry applications, preventing comparisons with modelled values.

5.4.2. Seasonal and Annual N_2O Emissions Modelled After Fall and Spring Slurry Applications

5.4.2.1. Fall Slurry Applications

NI greatly reduced N_2O emissions modelled from fall applications during autumn (16 Sep. – 31 Dec. in Table 6) in 2014 and 2015, slightly reduced N_2O emissions modelled during the following winter and early spring (1 Jan. – 30 Apr.), but slightly raised N_2O emissions modelled during the following summer (1 May – 15 Sep.) in both 2015 and 2016. Annual emissions modelled with NI were reduced from those without NI by 26% and 38% in 2014/2015 and 2015/2016 respectively (Table 6). The reduction modelled in 2014/2015 was similar to one of

23% estimated for DMPP from manual chamber measurements from 1 Oct. 2014 to 30 Sep. 2015 by Lin et al. (2018), although the reduction with NI modelled in 2015/2016 was greater than one of 15% estimated from manual chamber measurements from 1 Oct. 2015 to 30 Sep. 2016.

5.4.2.2. Spring Slurry Applications

Reductions in annual N_2O emissions modelled from spring slurry applications with DMPP and nitrapyrin occurred almost entirely during late spring and summer (1 May – 15 Sep. in Table 6). These reductions were 22% and 40% from those modelled without NI in 2014/2015 and 2015/2016 respectively (Table 6). The reduction modelled with NI in 2014/2015 was greater than one of 0% for DMPP estimated from manual chamber measurements from 1 Oct. 2014 to 30 Sep. 2015 by Lin et al. (2018), although the reduction modelled in 2015/2016 was similar to one of 38% estimated from manual chamber measurements from 1 Oct. 2015 to 30 Sep. 2016.

5.5. Effects of Management on Seasonal and Annual N_2O Emissions Modelled After Fall and Spring Slurry Applications

Advancing fall slurry application by 2 weeks increased N_2O emissions modelled with and without NI during autumn but reduced those during subsequent spring thaw (F -2 in Table 6) so that annual emissions modelled with and without NI were similar to those in F with the application dates in the experiment (Table 3). Delaying fall slurry application by 2 weeks reduced N_2O emissions modelled with and without NI only slightly during autumn, but greatly increased emissions modelled during subsequent spring thaw (F +2 in Table 6), particularly with the later fall application in 2016 (Table 3). Consequently delaying fall slurry application by 2 weeks caused substantial increases in annual N_2O emissions. However reductions in N_2O emissions modelled with NI in F +2 in 2015 and 2016 (34% and 47%) were greater than those in F (26% and 38%), because inhibition declined more slowly in colder soil (Eq. 1), particularly with later application in 2016.

Increasing surface litter incorporation and soil mixing during fall slurry application raised N_2O emissions modelled without NI only slightly during 2014/2015, but substantially during 2015/2016, particularly during spring thaw (F 0.5 and F 0.8 vs. F in Table 6). Increasing surface

litter incorporation and soil mixing during spring slurry application had limited effects on emissions (S 0.5 and S 0.8 vs. S in Table 6). Greater mixing caused reductions in N_2O emissions modelled with NI to be smaller relative to those without NI.

5.6. NI Effects on Annual Mineral N Losses and NH_3 Emissions

Injecting the slurry to 14 cm in the model suppressed NH_3 emissions with limited soil mixing, and caused only very small emissions with greater mixing (Table 7). Higher NH_4^+ concentrations modelled with NI (Fig. 2a,b) increased net NH_3 emission, particularly if fall slurry application was delayed or soil mixing was increased in 2014/2015.

The subhumid climate at Edmonton (Table 4) caused modelled NO_3^- losses to remain small. For both fall and spring applications, lower NO_3^- concentrations modelled with NI (Fig. 2c,d) caused small reductions in NO_3^- losses.

5.7. NI Effects on Barley Silage Yields

Silage yields modelled with fall slurry application were smaller than those measured in the drier year 2015, but those modelled with both applications were greater than those measured in the wetter year 2016, likely because of lodging observed in the field plots following the second year of heavy manure use (Table 8). Modelled yields were unaffected by NI for fall and spring applications in both years, although measured yields were raised by NI with spring application in 2015. Modelled yields were affected by the cutting height and harvest efficiency set in the model runs (Sec. 4.2).

6. DISCUSSION

6.1. Process Modelling of N_2O Emissions

N_2O emissions were driven by declines in gaseous O2 (O_{2g}) and O_{2s} modelled by equilibrating O_2 active uptake by autotrophic and heterotrophic oxidation (Sec. 2.5 step 3 and Sec. 2.3 step 3) with O_2 diffusion and dissolution through gaseous and aqueous phases, and dissolution from gaseous to aqueous phases, largely controlled by θ_g (Sec. 2.11 steps 1 – 3) (Fig. 1). These O_2 transfers were sustained by concentration gradients from O_{2g} to O_{2s} and from O_{2s} to O2 at microbial surfaces (O_{2m}), so that declines in O_{2s} (Fig. 3) and O_{2m} were relatively larger

than those in O_{2g}. These greater declines enabled N_2O emissions to be modelled from O_2 deficits while O_{2g} remained above one-half of atmospheric concentration, consistent with observations of O_{2g} during N_2O emissions from incubation and field experiments (Nguyen et al., 2017; Owens et al., 2017). These O_2 deficits were modelled using a K_m for O_{2m} of 10 μM by nitrifiers (Sec. 2.5 step 3) and 2 μM by denitrifiers (Sec. 2.3 step 3) derived from biochemical studies by Focht and Verstraete (1977). These K_m are less than 5% and 1% of atmospheric equivalent concentration, indicating the importance of explicitly simulating gaseous and aqueous transport processes ~~(Sec. 2.11)~~ when modelling N_2O emissions.

O_2 deficits were modelled in spring thaw 2015 (Fig. 3a), when diffusion was sharply reduced by soil saturation because drainage from snowmelt and soil thaw was impeded by underlying ice layers. These declines drove N_2O generation (Fig. 3b) and emission (Fig. 4b) almost entirely from NO_2^- reduced during spring thaw. O_2 deficits were also modelled during winter 2016 when increased θ_l from soil freezing with lower T_s under a shallower snowpack caused near-surface soil porosity to be fully occupied by ice and water. Consequent loss of θ_g greatly reduced surface gas exchange ~~(Sec. 2.11)~~ and hence gradually reduced soil O_2 concentrations, particularly with increased O_2 demand from fall slurry application (Fig. 3c). The extended period of low O_{2s} prolonged overwinter accumulation of N_2O_s after fall slurry application (Fig. 3d). Transient increases in θ_g during soil freeze-thaw cycles caused several N_2O emission events to be modelled during spring thaw in 2016, mostly from degassing through volatilization of overwinter N_2O_s (Fig. 5b) ~~(Sec. 2.11 step 1)~~. Degassing events in the model were consistent with field observations by Chantigny et al. (2017) that passive degassing of accumulated gases made a significant contribution to spring thaw emissions during which two or more consecutive emission peaks were often observed. In the model, the contribution by degassing of overwinter N_2O_s to spring thaw emissions increased with intensity and duration of soil freezing during the previous winter. N_2O emissions simulated during spring thaw were thus driven by concurrent NO_2^- reduction during spring thaw (2015) and by earlier NO_2^- reduction accumulated over the previous winter (2015/2016), as has been proposed from experimental observations (Teepe et al., 2004).

O_2 deficits were also caused by rapid increases in O_2 active uptake with addition of labile C in slurry, the rapid decomposition and oxidation of which (Sec. 2.3 step 1) caused transient declines in O_{2s} with soil wetting from slurry application and precipitation (Fig. 3e,g). After slurry application in the wetter spring of 2016, modelled O_{2g} declined to *ca*. one-half of atmospheric concentration, driving the sharp declines in O_{2s} shown in Fig. 3g. The modelled declines in O_{2g} were consistent with results from an incubation of wetted soil amended with cattle slurry by Nguyen et al. (2017) in which O_{2g} declined below one-half of atmospheric concentration within one day of slurry application and gradually rose again after two days, while no decline occurred in an unamended soil. The period of low O_{2s} in this incubation study co-incided with peak emissions of CO_2 and N_2O from the amended soil, as was modelled here in Fig. 3f,h and Fig. 6b and 7b. This co-incidence indicated that NH_4^+ and DOC oxidation drove O_2 deficits from demand for O_2 from oxidation vs. supply of O_2 through convection – dispersion, which caused NO_2^- reduction as represented in the model, again demonstrating the importance of simulating aqueous and gaseous O_2 transfers when modelling N_2O emissions.

6.2. Process Modelling of NI Effects on N_2O Emissions

6.2.1. Fall Slurry Application

NH_4^+ oxidation in the model (Sec. 2.5 step 4) proceeded rapidly after fall slurry application without NI as indicated by rapid declines in NH_4^+ (Fig. 2a), consistent with observations in other studies that soil NH_4^+ concentrations returned to background levels 30 d after fall slurry application (Rochette et al., 2004). Slower NH_4^+ oxidation modelled with NI (Eq. 3) during fall caused slower declines of soil NH_4^+ before and during freezing and hence larger NH_4^+ concentrations during spring thaw (Fig. 2a). These slower declines were modelled from slower decline of I_t with low f_{Ts} in cold soils (Eq. 1) which slowed NH_4^+ oxidation and thereby reduced N_2O emissions simulated during late autumn and spring thaw (Figs. 4b and 5b), despite increased NH_4^+ concentrations (Fig. ~~3~~2). These reductions were consistent with those from chamber measurements at the Edmonton South Farm (Lin et al., ~~2017~~2018), and with those from a limited number of studies elsewhere in which persistent effects of NI in reducing overwinter N_2O emissions have been found (e.g. Pfab et al., 2012), indicating the importance of f_{Ts} in Eq. 1.

878 The slower decline of I_t from low f_{Ts} enabled *ecosys* to simulate larger reductions in N_2O
879 emissions with NI after fall slurry applications in cooler soil vs. spring slurry applications in
880 warmer soil during both years (F during autumn *vs*. S during late spring-summer in Table 6).
881 Reductions in N_2O emissions modelled with NI after fall slurry applications became greater
882 when fall applications were delayed (F +2 in Table 6), further reducing T_s and f_{Ts} during
883 subsequent nitrification. The greater reductions modelled with fall applications were consistent
884 with experimental observations by Merino et al. (2005) who attributed larger reductions in N_2O
885 emissions measured with NI from fall- vs. spring-applied cattle slurry to slower NI degradation
886 in cooler soil. These modelled and experimental results indicated that NI effectiveness in
887 reducing N_2O emissions varies with the effect of fall slurry timing on f_{Ts}.
888
889 The greater reductions in N_2O emissions modelled from delayed fall applications with NI
890 were associated with much greater N_2O emissions modelled from delayed fall applications
891 without NI (F+2 in Table 6). These greater emissions were attributed to less NH_4^+ oxidation
892 before freeze up in fall, resulting in more NH_4^+ remaining to drive NH_4^+ oxidation and hence
893 N_2O emissions during spring thaw. These model findings were consistent with field results from
894 Chantigny et al. (2017) in Quebec, and Kariyapperuma et al. (2012) in Ontario, where greater
895 spring N_2O emissions were measured when fall slurry was applied in late November than in
896 early November. These greater spring thaw N_2O emissions were attributed by Kariyapperuma et
897 al. (2012) to greater mineral N concentrations during spring thaw caused by less nitrification
898 before freeze up during the previous fall, as modelled here. The greater N_2O emissions modelled
899 with later slurry application were also driven by more rapid DOC oxidation from more labile
900 manure C remaining during spring thaw. ~~that~~ This more labile manure C reduced [O_{2s}] below
901 that simulated after earlier fall applications (Fig. 3d). NI may therefore be particularly effective
902 in reducing N_2O emissions during spring thaw following late fall slurry applications.
903
904 The decreases in N_2O emissions modelled with NI from greater soil mixing (F 0.5 and F 0.8
905 *vs*. F in Table 6) were affected by how the redistribution of NI activity with soil mixing was
906 modelled. Simulating this redistribution during tillage requires further consideration and
907 corroboration from observations. These decreases in N_2O emissions with NI were associated
908 with greater N_2O emissions modelled from greater soil mixing without NI in 2016 (F 0.5 and F

0.8 in Table 6). These greater emissions were attributed in the model to longer periods with high θ_i and low θ_g in the upper soil profile caused by greater heat loss through reduced insulation from less surface litter under a shallow snow pack [D12, D13]. This longer period further reduced overwinter [O_{2s}] from that modelled in F (Fig. 3c), causing greater accumulation of N_2O_s and hence greater emissions during thaw. These model findings were consistent with field observations by Congreves et al. (2017) and Wagner-Riddle et al. (2010) that overwinter N_2O emissions increased with greater freezing under conventional vs. no tillage, particularly with surface residue removal. Model findings were also consistent with observations by Teepe et al. (2004) that N_2O emissions during soil thawing rose sharply with increased duration of soil freezing. Consequent changes in T_s with freezing may alter NI effectiveness with tillage.

6.2.2. Spring Slurry Application

Annual N_2O emissions modelled without NI from spring applications were smaller than those from fall applications in 2014/2015 with a wetter early spring and drier late spring, and slightly greater in 2015/2016 with a drier early spring and wetter late spring (Table 4), except when fall application was delayed (e.g. F +2 in Table 6). These modelled differences in emissions were consistent with experimental findings that drier springs reduce N_2O emissions from fall applications relative to those from spring (e.g. Cambareri et al., 2017). These model results indicate that effects of spring vs. fall slurry applications on annual N_2O emissions may not be consistent, but rather will depend on the timing of fall application relative to freeze up, and on precipitation during the following winter and spring.

Amendment of slurry with NI slowed declines in NH_4^+ modelled after spring applications comparably to those measured (Fig. 2b). These slower declines were caused by slower NH_4^+ oxidation that reduced nitrifier growth (Sec. 2.9 Eq. 3) and active O_2 uptake (Sec. 2.5 step 3). Consequently smaller nitrifier biomass and greater [O_{2s}] were modelled with *vs*. without NI (Fig. 3e,g), particularly with rainfall after spring application in 2016 (Fig. 7a). The smaller nitrifier biomass modelled with NI was consistent with the findings of Dong et al. (2013) that DMPP reduced populations of ammonia oxidizing bacteria in soil incubations. Greater [O_{2s}] modelled with NI was consistent with greater [O_{2g}] measured in an incubation of wetted soil amended with cattle slurry with *vs*. without DMPP by Nguyen et al. (2017). Slower nitrifier growth and greater

940 [O_{2s}] both contributed to reductions in N_2O emissions modelled with NI beyond those from the
941 direct effects of I_t on nitrification in Eq. 1, indicating additional effects of NI on N_2O emissions
942 that should be considered in NI models.
943
944 The reductions in N_2O emissions modelled for 30 d after spring slurry applications with R_I
945 for DMPP and nitrapyrin in 2015 (35% and 30%) and 2016 (53% and 41%) were less than those
946 measured with automated chambers (Table 5), but within the range of 31% to 44% in meta-
947 analyses of NI research by Akiyama et al. (2010) and Ruser and Schultz (2015). The greater
948 reductions modelled in 2016 *vs*. 2015 (Fig. 7 *vs*. Fig. 6) were consistent with findings in meta-
949 analyses by Akiyama et al. (2010) and Gilsanz et al. (2016) that NI was more effective in
950 reducing N_2O emissions from a given land use when emissions were greater. These greater
951 reductions were attributed in the model to heavy rainfall several days after application in 2016
952 (Fig. 7a) that extended the N_2O emission period (Fig. 7b). During this extension I_t remained high
953 because [NH_4^+] had declined from the large values modelled immediately after application (Eq.
954 3).
955
956 The effects of NI on N_2O emissions modelled with greater soil mixing during spring
957 applications (S 0.5 and S 0.8 *vs*. S in Table 6) were affected by how the redistribution of NI
958 activity with soil mixing was modelled, as were those during fall applications. The effects of soil
959 mixing on N_2O emissions without NI modelled from slurry applications in spring were smaller
960 than those in fall in the absence of soil freezing effects on O_{2s}. These smaller effects were
961 modelled because tillage in this study involved mixing of injected manure rather than
962 incorporation of surface-applied manure. These small effects were consistent with an observation
963 by VanderZaag et al. (2011) that tillage was less important than timing and placement for N_2O
964 emissions from slurry applications.
965
966 The reductions in annual N_2O emissions modelled after spring slurry applications with R_I for
967 DMPP and nitrapyrin in 2015 (22% and 17%) and 2016 (40% and 27%) (Table 6) were smaller
968 than those modelled after 30 d (Table 5) due to gradual degradation of NI effectiveness modelled
969 with time since application (Eq. 1), indicating the importance of year-round modelling and
970 measurements to fully assess NI effects on N_2O emission factors for IPCC Tier 3 methodology.

971 However most of the datasets used in meta-analyses of these assessments did not include
972 emissions during autumn, winter and spring thaw (Ruser and Schulz, 2015) which are
973 particularly important for estimating emission factors for NI effects from fall slurry applications
974 in cold climates (Table 6). Ecosystem modelled with well tested simulation of NI effects may
975 make a valuable contribution to these assessments.
976
977 **6.3.Modelling NI Effects on NH_3 Emissions and Mineral N Losses**
978 The small NH_3 emissions modelled from slurry injection with limited soil mixing (Table 7)
979 were consistent with observations of almost no NH_3 volatilization from closed-slot injection of
980 slurry by Rodhe et al. (2006). In the model, NH_3 emissions with or without NI were sharply
981 reduced by NH_4^+ adsorption ~~(Sec. 2.10)~~ with diffusion of NH_3 and NH_4^+ from the injection site
982 ~~(Sec. 2.11)~~. Greater soil mixing brought more NH_4^+ closer to the surface, reducing NH_4^+
983 adsorption and thereby increasing NH_3 emission, particularly from fall applications with NI
984 (Table 7). Consequently only small net increases in NH_3 emissions (Table 7) were modelled
985 with NI from increased volatilization of aqueous NH_3 ~~(Sec. 2.11 step 1)~~ in equilibrium with
986 increased NH_4^+ concentrations (Fig. 2). However these increases were large in relative terms
987 particularly following fall applications, consistent with increases of 33 – 67% and 3 – 65%
988 relative to emissions without NI derived from meta-analyses of field experiments by Qiao et al.
989 (2015) and Lam et al. (2017) respectively. Increases in NH_3 emissions with NI will thus depend
990 on soil adsorptive properties and depth of slurry incorporation.
991
992 The small losses of NO_3^-, and consequently the small reductions in these losses with NI,
993 modelled in the subhumid climate at the Edmonton South Farm (Table 7) conform to the
994 assumption by De Klein et al. (2006) that NO_3^- leaching is an insignificant source of indirect
995 N_2O emission from dryland cropping systems in subhumid climates. Consequently reductions in
996 leaching have minimal impact on the overall effect of NI on N_2O emission in these climates
997 (Lam et al., 2017). Reductions in NO_3^- losses modelled with NI would be larger at sites with
998 better drainage and more excess precipitation, although even under these conditions such
999 reductions may be small and inconsistent (Smith et al., 2002).
1000

The increases in NH_3 emissions modelled with NI were larger than reductions in NO_3^- leaching (Table 7), indicating that net increases in N_2O emissions from indirect effects of NI will partially offset decreases in N_2O emissions from direct effects. This offset must be included when estimating changes in N_2O emission factors attributed to NI in IPCC Tier 3 methodology.

6.4. Modelling NI Effects on N_2O Emissions: Parameter Evaluation

The simulation of N_2O emissions from nitrification and denitrification in *ecosys* is based on a comprehensive representation of biological and physical processes governing production and transport of N_2O. Parameters used in these processes are well constrained from basic research so that the model may provide a robust means to predict emissions under diverse climates, soils and land use practices. These processes in *ecosys* were not changed when adding the algorithm for inhibiting NH_4^+ oxidation by nitrifiers proposed in Eqs. 1 and 2 (Sec. 2.9). This algorithm used only three parameters, $I_{t=0}$ and R_I in Eq. [1] and K_{iNH4} in Eq. [2] with values of 1.0, 2.0 x 10^{-4} h^{-1}, and 7000 g N m^{-3} to simulate the time course of NI activity following slurry application. The first two parameters correspond to ones in earlier models of NI for inhibition effectiveness (0.5 – 0.9) and duration (30 – 60 days) (Cui et al., 2014; Del Grosso et al., 2009). These models have given reductions in N_2O emissions with NI in agricultural crops of *ca*. 25% (Cui et al., 2014), 10% (Del Grosso et al., 2009) or less (Abalos et al., 2016), that are frequently smaller than reductions of 26% – 43% and 24% – 46% derived from meta-analyses of NI effects in agricultural crops by Akiyama et al. (2010) and Gilsanz et al. (2016) respectively. Direct effects on NI of soil water content and pH were not modelled here due to uncertainty in parameterization, although both affect nitrification and hence the magnitude of NI activity.

Each of the parameters used to model NI in *ecosys* requires further evaluation. A larger R_I, such as that used for nitrapyrin *vs*. DMPP (Sec. 2.9), caused a more rapid decline of NI activity in soil, and hence greater N_2O emissions with time after slurry application that were consistent with measurements (Tables 5 and 6; Lin et al., 2018). This larger value might represent more rapid degradation of nitrapyrin through volatilization (Ruser and Schulz, 2015), although meta-analyses of N_2O reductions with NI indicate that those with nitrapyrin are similar to those with DMPP. The value of R_I used for NI in the model will thus likely be product specific. The effect of T_s on R_I might reasonably be represented by f_{Ts} as is the effect of T_s on all other biological

reactions in the model. This function allowed modelled NI activity to persist overwinter (Fig. 2) and hence reduce N_2O emissions modelled during spring thaw (Fig. 6 and Fig. 7). However the effects of temperature on reductions in N_2O emission with NI over time are sometimes unclear in controlled studies (Kelliher et al., 2008).

The value of $I_{t=0}$ set the value of I_t at the time of slurry application, after which I_t underwent first order decline over time according to Eq. 1 (Sec. 2.9). The current value of 1.0 indicates complete inhibition at the time of application, but might be reduced if the amount of NI at application is less than that required for complete inhibition. However I_t had to remain large enough to reduce N_2O emissions from nitrification for several weeks after application (Figs. 6 and 7) even with higher soil NH_4^+ concentrations (Fig. 2). Lowering $I_{t=0}$ from 1.0 to 0.8, similar to that in earlier NI models in which I_t decline was not simulated, increased N_2O emissions modelled over 30 days after spring slurry applications by 7% in 2015 and 25% in 2016 (Table 9).

The value of K_{iNH4} in Eq. 2 reduced I_t with the very large NH_4^+ concentrations modelled immediately after injecting slurry with large NH_4^+ content (Table 3) into small bands (Sec. 3.1). The use of K_{iNH4} was suggested by the findings of Janke et al. (2019) that NI may not have the expected impacts on N transformations and availability when applied in a concentrated band with large NH_4^+ concentrations (up to 12 kg N Mg^{-1}), similar to those modelled immediately after slurry application in this study. The modelled NH_4^+ concentrations declined rapidly after application through diffusion ~~(Sec. 2.11)~~, adsorption ~~(Sec. 2.10)~~ and nitrification (Sec. 2.5), and thus so did K_{iNH4} effects on inhibition. The value of K_{iNH4} in Eq. 2 therefore governed NI effects modelled during the brief periods of rapid N_2O emissions following application (*ca*. 3 days in Figs. 6 and 7), but had sharply diminishing impacts on NI effects modelled thereafter. An alternative hypothesis for reduced inhibition by NI immediately after application might be more rapid diffusion of NH_4^+ than NI from the band, leading to spatial separation (Ruser and Schulz, 2015), although parameterization of this hypothesis is uncertain. Halving or doubling K_{iNH4} from the value set in Sec. 2.9 raised or lowered N_2O emissions modelled over 30 days after spring slurry applications by 7 – 8% in 2015 and 2016 (Table 9), indicating some latitude in evaluating this parameter.

Reductions in N_2O emissions modelled with all proposed values of $I_{t=0}$ and K_{iNH4} varied from 27% to 41% in 2015, and from 38% to 57% in 2016 (Table 9), close to the range of 42.6% ± 5.5% derived from meta-analyses of NI effects with cattle slurry by Gilsanz et al. (2016). Further evaluation of these parameters should be undertaken in future studies in which measurements are taken at higher frequencies (e.g. Figs. 6 and 7) required to assess N_2O emissions and NI effects on them.

6.5.Modelling NI Effects on N_2O Emissions: Outstanding Issues

Several issues remain to be addressed in modelling N_2O emissions and NI effects on these emissions. Accurately modelling emissions during spring thaw depended upon accurately modelling soil freezing and thawing following snow melt, and their effects on soil O_2 transfer. A small delay of 2 – 3 days in modelled thawing caused some small emission events measured in early spring of 2015 to be missed (Fig. 4b). However because modelled emissions were driven by overwinter accumulation of N_2O (Fig. 3), seasonal emissions were less affected by such delays than were emissions from individual events. Algorithms for modelling snowpack accumulation and ablation in *ecosys* are being further refined to improve simulation of soil freezing and thawing. Accurately modelling emissions during later spring depended upon accurately modelling soil wetting and drying following rainfall, and their effects on soil O_2 transfer. Soil wetting from heavy precipitation typically drives N_2O emission events following soil N additions, as modelled here during DOY 143 – 146 in 2016, although such events were not always measured (Fig. 7b). Such wetting caused sharp declines in O_{2s} when soil water content rose above a critical threshold, driving N_2O generation and subsequent emission (Fig. 3). However modelling these thresholds depends on soil hydrological properties used in the model (Table 2) which may not be known with sufficient accuracy.

Modelling NI effects on N_2O emissions depended upon $I_{t=0}$ (Eq. 1) and K_{iNH4} (Eq. 2) as evaluated in Sec. 6.4 and Table 9, but also on the time course for declining NI activity governed by the first order rate constant R_I and its temperature dependence f_{Ts_I} (Eq. 1). NI activity modelled with R_I and f_{Ts_I} in this study reduced nitrification alone (Sec. 2.9), which enabled higher $[NH_4^+]$ and lower $[NO_3^-]$, and hence greater NH_3 emissions, to be simulated with NI after amendment as has been found in field studies (Fig. 2). These higher $[NH_4^+]$ required a low value

Formatted: Subscript
Formatted: Subscript
Formatted: Subscript
Formatted: Subscript
Formatted: Subscript
Formatted: Subscript
Formatted: Subscript
Formatted: Subscript
Formatted: Indent: First line: 0.25"
Formatted: Subscript
Formatted: Superscript
Formatted: Subscript
Formatted: Superscript
Formatted: Subscript

of R_I so that NI activity would persist in reducing nitrification and hence N_2O emissions after soil amendment. This model of NI activity contrasted with that in a more complex model in which NI reduced N_2O emissions directly, rather than through nitrification (Li et al., 2020). In such a model, NI would not directly affect $[NH_4^+]$ and $[NO_3^-]$ so that greater values of R_I could be used to get similar reductions in N_2O emissions. The values of R_I and $f_{Ts,I}$ used in our model caused N_2O emissions modelled with NI to decline more rapidly than those measured following spring applications (Fig. 6b and Fig. 7b). These values need to be constrained by further studies with more frequent measurements of declines in NI activity following amendment to determine if alternative models for the time course of these declines might be considered.

Formatted: Subscript

Formatted: Subscript

Formatted: Subscript

Formatted: Subscript

7. CONCLUSIONS

(a) A simple, time-dependent algorithm for adding NI effects on N_2O emissions into the existing model *ecosys* has been presented.

(b) The direct effect of NI on N_2O emissions in the model was confined to the inhibition of NH_4^+ oxidation

(c) Additional effects of NI on N_2O emissions were caused by slower nitrifier growth and O_2 uptake. The combined effects in (b) and (c) reduced N_2O emissions by 35% - 58% depending on seasonal weather and time of manure application.

Formatted: Subscript

(d) Slower nitrification modelled with this algorithm caused increases in soil NH_4^+ concentrations and reductions in soil NO_3^- concentrations and N_2O fluxes that were consistent with those measured following fall and spring applications of slurry over two years.

(e) NI in the model remained effective in reducing N_2O emissions modelled during spring thaw, particularly when these emissions were increased by delaying fall slurry applications or increasing fall tillage intensity

(f) NI in the model increased NH_3 emissions more than it reduced NO_3^- leaching, causing indirect effects on N_2O emissions that partially offset direct effects.

(g) NI had no significant effect on modelled or measured barley silage yields.

(h) Some further work is needed to corroborate parameters in the NI algorithm under a wider range of site conditions.

(i) The addition of NI to *ecosys* may allow emission factors for different NI products to be derived from annual N_2O emissions modelled under diverse site, soil, land use and weather as required in IPCC Tier 3 methodology.

ACKNOWLEDGEMENTS

High performance computing facilities for *ecosys* were provided by Compute Canada (www.computecanada.ca) through the WestGrid computing network (https://www.westgrid.ca). Field measurements were supported by the Alberta Livestock and Meat Agency Ltd. (2014E017R), Climate Change and Emissions Management Corporation (0019083), Dow AgroSciences (0022950), and Eurochem Agro (0027592).

LIST OF REFERENCES

Abalos , D., Smith, W.N., Grant, B.B., Drury, C.F., MacKell, S. and Wagner-Riddle, C.: Scenario analysis of fertilizer management practices for N_2O mitigation from corn systems in Canada. Science of the Total Environ. 573, 356–365, 2016.

Akiyama, H., Yan, X. and Yagi, K.: Evaluation of effectiveness of enhanced efficiency fertilizers as mitigation options for N2O and NO emissions from agricultural soils: Meta-analysis. Glob. Change Biol. 16,1837–1846. doi:10.1111/j.1365-2486.2009.02031.x, 2010.

Cambareri, G., Drury, C., Lauzon, J., Salas, W. and Wagner-Riddle, C.: Year-round nitrous oxide emissions as affected by timing and method of dairy slurry application to corn. Soil Sci. Soc. Am. J. 81, 166–178, 2017.

Chantigny, M.H., Rochette, P., Angers, D.A., Goyer,C., Brin, L.D. and Bertrand. N.: Nongrowing season N_2O and CO_2 emissions − Temporal dynamics and influence of soil texture and fall-applied slurry. Can. J. Soil Sci. 97(3), 452-464, 2017.

Congreves, K.A., Brown, S.E., Németh, D.D., Dunfield K.E. and Wagner-Riddle, C.: Differences in field-scale N_2O flux linked to crop residue removal under two tillage systems in cold climates. GCB Bioenergy 9, 666–680, doi: 10.1111/gcbb.12354, 2017.

Cui, F., Zheng, X., Liu, C., Wang, K., Zhou, Z. and Deng, J.: Assessing biogeochemical effects and best management practice for a wheat–maize cropping system using the DNDC model. Biogeosci. 11, 91–107, 2014.

De Klein C., Novoa, R.S.A., Ogle, S. et al.: N_2O emissions from managed soils, and CO_2 emissions from lime and urea application. Chapter 11. In: 2006 IPCC Guidelines for National Greenhouse Gas Inventories (eds Eggleston HS, Buendia L, Miwa K, Ngara T, Tanabe K). IGES, Hayama, Japan, 2006.

Del Grosso, S.J., Ojima, D.S., Parton, W.J., Stehfest, E., Heistemann , M., DeAngelo, B. and Rose, S.: Global scale DAYCENT model analysis of greenhouse gas emissions and mitigation strategies for cropped soils. Global and Planetary Change 67, 44–50, 2009.

Dong, X.X., Zhang, L.L., Wu, Z.J., Zhang, H.W. and Gong, P.: The response of nitrifier, N-fixer and denitrifier gene copy numbers to the nitrification inhibitor 3,4-dimethylpyrazole phosphate . Plant, Soil Environ. 59(9), 398-403, 2013

Dungan, R.S., Leytem, A.B., Tarkalson, D.D., Ippolito, J.A. and Bjorneberg, D.L.: Dairy forage rotation as influenced by fertilizer and slurry applications. Soil Sci. Soc. Amer. J. 81, 537–545, 2017.

Focht, D.D. and Verstraete, W.: Biochemical ecology of nitrification and denitrification. Adv. Micro. Ecol. 1, 135-214, 1977.

Gao, W. and Bian, X.: Evaluation of the agronomic impacts on yield-scaled N_2O emission from wheat and maize fields in China. Sustainability 9, 1201; doi:10.3390, 2017.

Gilsanz, C., Báez, D., Misselbrook,T.H., Dhanoa, M.S. and Cárdenas, L.M.: Development of emission factors and efficiency of two nitrification inhibitors, DCD and DMPP. Agric, Ecosyst. Environ. 216, 1-8, 2016.

Giltrap, D.L., Saggar, S., Singh, J., Harvey, M., McMillan, A, and Laubach, J.: Field-scale verification of nitrous oxide emission reduction with DCD in dairy-grazed pasture using measurements and modelling. Soil Res. 49, 696–702 http://dx.doi.org/10.1071/SR11090, 2011.

Grant, R.F.: A technique for estimating denitrification rates at different soil temperatures, water contents and nitrate concentrations. Soil Sci. 152, 41-52, 1991

Grant, R.F.: Simulation of ecological controls on nitrification. Soil Biol. Biochem. 26, 305-315, 1994.

Grant, R.F.: Mathematical modelling of nitrous oxide evolution during nitrification. Soil Biol. Biochem. 27, 1117-1125, 1995.

Grant, R.F. and Pattey, E.: Mathematical modelling of nitrous oxide emissions from an agricultural field during spring thaw. Global Biogeochem. Cycles. 13, 679-694, 1999.

Grant, R.F. and Pattey, E.: Temperature sensitivity of N_2O emissions from fertilized agricultural soils: mathematical modelling in *ecosys*. Global Biogeochem. Cycles 22, GB4019, doi:10.1029/2008GB003273, 2008.

Grant, R.F., Pattey, E.M., Goddard, T.W., Kryzanowski, L.M. and Puurveen, H. Modelling the effects of fertilizer application rate on nitrous oxide emissions from agricultural fields. Soil Sci Soc. Amer. J. 70,~~:~~ 235-248, 2006.

Grant, R.F., Neftel, A. and Calanca, P.: Ecological controls on N_2O emission in surface litter and near-surface soil of a managed pasture: modelling and measurements. Biogeosci. 13, 3549–3571, 2016.

Guardia, G., Cangani, M.T., Sanz-Cobena, A., Junior, J.L. and Vallejo, A.: Management of pig slurry to mitigate NO and yield-scaled N_2O emissions in an irrigated Mediterranean crop. Agric. Ecosyst. Environ. 238, 55-66, 2017.

Guardia, G., Marsden, K.A., Vallejo, A., Jones, D.L. and Chadwick, D.R.: Determining the influence of environmental and edaphic factors on the fate of the nitrification inhibitors DCD and DMPP in soil. Sci. Total Environ. 624, 1202-1212, 2018.

IPCC. 2019. 2019 Refinement to the 2006 IPCC guidelines for national greenhouse gas inventories. https://www.ipcc.ch/. accessed 9 July 2019.

Janke, C.K., Fujinuma, R., Moody, P. and Bell, M.J.: Biochemical effects of banding limit the benefits of nitrification inhibition and controlled-release technology in the fertosphere of high N-input systems. Soil Res. 57, 28–40 https://doi.org/10.1071/SR18211, 2019.

Kariyapperuma, K. A., Furon, A. and Wagner-Riddle, C.: Non-growing season nitrous oxide fluxes from an agricultural soil as affected by application of liquid and composted swine slurry. Can. J. Soil Sci. 92, 315,327, 2012.

Kelliher, F. M., Clough, T.J., Clark, H., Rys, G. and Sedcole, J.R.: The temperature dependence of dicyandiamide (DCD) degradation in soils: a data synthesis. Soil Biol. Biochem. 40, 878–1882, 2008.

Lam S.K., Suter, H., Mosier, A.R. and Chen, D.: Using nitrification inhibitors to mitigate agricultural N_2O emission: a double-edged sword? Global Change Biol. 23, 485–489, 2017.

Lam, S.K., Suter, H., Davies, R., Bai, M., Mosier, A.R., Sun, J. and Chen, D.: Direct and indirect greenhouse gas emissions from two intensive vegetable farms applied with a nitrification inhibitor. Soil Biol. Biochem. 116, 48-51, 2018.

Li, Y., Shah, S.H.H. and Wang, J.: Modelling nitrification inhibitor effects on emissions of nitrous oxide (N_2O) in the UK, Science of The Total Environment, 709: 136156, 2020.

Lin, S., Hernandez-Ramirez, G., Kryzanowski, L., Wallace, T., Grant, R., Degenhardt, R., Berger, N., Lohstraeter , G. and Powers, L.-A.: Timing of Slurry Injection and Nitrification Inhibitors Impacts on Nitrous Oxide Emissions and Nitrogen Transformations in a Barley Crop. Soil Sci. Soc. Amer. J. 81,1595-1605 doi:10.2136/sssaj2017.03.0093, 2018.

Merino, P., Menéndez, S., Pinto, M., González-Murua, C. and Estavillo, J.M.: 3, 4-Dimethylpyrazole phosphate reduces nitrous oxide emissions from grassland after slurry application. Soil Use Manage. 21, 53–57, 2005.

Metivier, K.A., Pattey, E. and Grant, R.F.: Using the *ecosys* mathematical model to simulate temporal variability of nitrous oxide emissions from a fertilized agricultural soil. Soil Biol. Biochem. 41, 2370–2386, 2009.

Nguyen, Q.V., Wu, D., Kong, X., Bol, R., Petersen, S.O., Jensen, L.S., Liu, S., Brüggemann, N., Glud, R.N., Larsen, M. and Bruun, S.: Effects of cattle slurry and nitrification inhibitor application on spatial soil-dynamics and N_2O production pathways. Soil Biol. Biochem. 11, 200-209, 2017.

Owens, J., Clough, T.J., Laubach, J., Hunt, J.E. and Venterea, R.T.: Nitrous oxide fluxes and soil oxygen dynamics of soil treated with cow urine. Soil Sci. Soc. Amer. J. 81, 289-298, doi:10.2136/sssaj2016.09.0277, 2017.

Formatted: Subscript

Qiao C., Liu, L., Hu, S., Compton, J.E., Greaver, T.L. and Li, Q.: How inhibiting nitrification affects nitrogen cycle and reduces environmental impacts of anthropogenic nitrogen input. Global Change Biol. 21,1249–1257, 2015.

Pfab, H., Palmer, I., Buegger, F., Fiedler, S., Muller, T. and Ruser, R.: Influence of a nitrification inhibitor and of placed N-fertilization on N_2O fluxes from a vegetable cropped loamy soil. Agric. Ecosyst. Environ. 150, 91– 101, 2012.

Rochette, P., Angers, D.A., Chantigny, M.H., Bertrand, N. and Côté, D.: Carbon dioxide and nitrous oxide emissions following fall and spring applications of pig slurry to an agricultural soil. Soil Sci. Soc. Amer. J. 68,1410–1420, 2004.

Rodhe, L., Pell, M. and Yamulki, S.: Nitrous oxide, methane and ammonia emissions following slurry spreading on grassland. Soil Use Manage. 22, 229–237. doi:10.1111/j.1475-2743.2006.00043.x, 2006.

Ruser, R. and Schulz, R.: The effect of nitrification inhibitors on the nitrous oxide (N_2O) release from agricultural soils—a review. J. Plant Nutr. Soil Sci. 178, 171–188, 2015.

Saxton, K.E., Rawls, W.J., Romberger, J.S. and Papendick, R. I.: Estimating generalized soil-water characteristics from texture. Soil Sci. Soc. Amer. J. 50(4), 1031-1036, 1986.

Smith, K. A., Beckwith, C. P., Chalmers, A. G., Jackson, D. R.: Nitrate leaching following autumn and winter application of animal manures to grassland. Soil Use Manage. 18, 428–434, 2002.

Subbarao G.V., Ito, O., Sahrawat, K.L. et al.: Scope and strategies for regulation of nitrification in agricultural systems: challenges and opportunities. Crit. Rev. Plant Sci. 25, 303–335, 2006.

Teepe, R., Vor, A., Beese, F. and Ludwig, B.: Emissions of N_2O from soils during cycles of freezing and thawing and the effects of soil water, texture and duration of freezing. Euro. J. Soil Sci. 55, 357–365, 2004.

VanderZaag, A.C., Jayasundara, S. and Wagner-Riddle, C.: Strategies to mitigate nitrous oxide emissions from land applied manure. Animal Feed Sci. Tech. 166–167, 464-479, 2011.

Wagner-Riddle, C., Rapai, J., Warland, J. and Furon, A.: Nitrous oxide fluxes related to soil freeze and thaw periods identified using heat pulse probes. Can. J. Soil Sci. 90, 409-418, 2010.

1265 Wagner-Riddle, C. and Thurtell, G.W.: Nitrous oxide emissions from agricultural fields during
1266 winter and spring thaw as affected by management practices. Nutr. Cycl. Agroecosyst.
1267 52, 151–163, 1998.
1268 Zhu, K., Bruun, S. and Jensen, L.S.: Nitrogen transformations in and N_2O emissions from soil
1269 amended with slurry solids and nitrification inhibitor. Euro. J. Soil Sci. 67, 792–803.
1270 2016.

Table 1: List of supplements in the Supporting Material

Supplement	Title	Equations
S1	Microbial C, N and P Transformations	[A1] – [A39]
S2	Soil-Plant Water Relations	[B1] – [B14]
S3	Gross Primary Productivity, Autotrophic Respiration, Growth and Litterfall	[C1] – [C53]
S4	Soil Water, Heat, Gas and Solute Fluxes	[D1] – [D21]
S5	Solute Transformations	[E1] – [E57]
S6	Symbiotic N_2 Fixation	[F1] – [F26]
S7	CH_4 Production and Consumption	[G1] – [G27]
S8	Inorganic N Transformations	[H1] – [H21]

1271

Table 2: Key soil properties of the Black Chernozem soil at the South Edmonton Farm used in *ecosys*.

Depth	BD	FC	WP	Ksat[1]	Sand	Silt	Clay	pH	SOC	SON
m to bottom	Mg m^{-3}	m^3 m^{-3}		mm h^{-1}	g kg^{-1} mineral soil				g kg^{-1} soil	
0.01	1.15	0.34	0.15	18.0	280	450	270	6.3	57.1	5.74
0.025	1.15	0.34	0.15	18.0	280	450	270	6.3	57.1	5.74
0.05	1.15	0.34	0.15	18.0	280	450	270	6.3	57.1	5.74
0.10	1.15	0.34	0.15	18.0	280	450	270	6.3	57.1	5.74
0.15	1.35	0.34	0.15	18.0	280	450	270	6.3	40.7	3.80
0.30	1.40	0.34	0.15	7.5	250	470	280	6.3	40.7	3.80
0.60	1.50	0.35	0.17	2.5	270	420	310	7.1	3.2	0.3
0.90	1.50	0.35	0.17	2.5	270	420	310	7.1	3.2	0.3
1.20	1.50	0.35	0.17	2.5	270	420	310	7.1	3.2	0.3
1.50	1.50	0.35	0.17	2.5	270	420	310	7.1	3.2	0.3

[1] from Saxton et al. (1986)

Formatted: Superscript

Formatted: Superscript

Table 3. Plant and soil management schedule at the Edmonton South Campus Farm

Year	Date	Management	Amount			
			---------- g N m^{-2} ----------			g C m^{-2}
			Urea	NH_4^+	Organic N	Organic C
2014	15 May	fertilizer	7.2			
	15 May	planting				
	21 Aug.	harvest				
	30 Sep.	fall slurry		21.7	16.4	229.4
2015	11 May	planting				
	12 May	spring slurry		19.4	20.5	176.9
	28 Jul.	harvest				
	07 Oct.	fall slurry		21.3	19.0	198.5
2016	14 May	planting				
	16 May	spring slurry		27.2	18.6	227.5
	15 Aug.	harvest				

Table 4. Average temperatures and total precipitation measured at the Edmonton South Farm during autumn/winter, winter/spring and spring/summer in 2014/2015 and 2015/2016.

	2014	2015		2014/5		2015	2016		2015/6
from	16 Sep	1 Jan	1 May	Average		16 Sep	1 Jan	1 May	Average
to	31 Dec	30 Apr	15 Sep	or Total		31 Dec	30 Apr	15 Sep	or Total
Temp. (ºC)	0.4	-1.8	16.0	**5.6**		0.8	0.1	15.8	**6.3**
Precip. (mm)	50	75	195	**320**		41	38	402	**481**

Table 5: Seasonal N_2O emissions measured and modelled during late spring in 2015 and 2016 without slurry (C) or with slurry applied in spring (S) without NI, with nitrapyrin or with DMPP on dates in the field study (Table 3). Negative values denote emissions, positive values uptake.

	Year	2015		2016	
	Period	12 May – 11 June		17 May – 16 June	
		Measured	Modelled	Measured	Modelled
Treat.	Amend.	---------- mg N m^{-2} ----------			
C		+3	-1	+14	-5
S	none	-88	-89	-160	-153
S	DMPP	-48	-58	-45	-72
S	nitrapyrin	-56	-62	-57	-91

Table 6: Seasonal and annual N_2O emissions modelled during autumn/winter, winter/spring and spring/summer in 2014/2015 and 2015/2016 without slurry (C) or with slurry applied in fall (F) or spring (S) without NI or with $\underline{R}_I$ for DMPP on dates in the field study (Table 3), and in fall on dates 2 weeks before (F-2) or after (F+2) those in the field study, and with soil mixing during slurry application (M) increased to 0.4 and 0.6 from 0.2 in the field study. Negative values denote emissions.

	Year	2014	2015		2014/5	2015	2016		2015/6
	from	16 Sep	1 Jan	1 May	Total	16 Sep	1 Jan	1 May	Total
	to	31 Dec	30 Apr	15 Sep		31 Dec	30 Apr	15 Sep	
Treat.	Amend.	---------- mg N m^{-2} ----------							
C		-2	-10	-14	**-26**	-2	-11	-13	**-26**
F	none	-93	-74	-17	**-184**	-93	-74	-27	**-194**
F	DMPP	-39	-68	-29	**-136**	-41	-50	-30	**-121**
F	nitrapyrin	-50	-101	-20	**-171**	-48	-61	-29	**-136**
S	none	-2	-10	-119	**-131**	-3	-25	-182	**-210**
S	DMPP	-2	-10	-90	**-102**	-3	-18	-106	**-127**
S	nitrapyrin	-2	-10	97	**-109**	-3	-24	-126	**-153**
F -2	none	-102	-64	-17	**-183**	-137	-47	-26	**-210**
F -2	DMPP	-56	-63	-19	**-138**	-55	-34	-23	**-112**
F +2	none	-92	-111	-17	**-220**	-84	-189	-52	**-325**
F +2	DMPP	-28	-78	-39	**-145**	-29	-99	-43	**-171**
F 0.5	none	-97	-71	-16	**-184**	-93	-168	-22	**-283**
F 0.5	DMPP	-58	-77	-17	**-152**	-59	-111	-20	**-190**
F 0.8	none	-102	-81	-21	**-204**	-98	-184	-19	**-301**
F 0.8	DMPP	-65	-76	-18	**-159**	-69	-138	-18	**-225**
S 0.5	none	-2	-10	-129	**-141**	-3	-27	-168	**-198**
S 0.5	DMPP	-2	-10	-98	**-110**	-3	-21	-124	**-147**
S 0.8	none	-2	-10	-138	**-150**	-3	-25	-168	**-196**
S 0.8	DMPP	-2	-10	-102	**-114**	-3	-19	-123	**-145**

Table 7: Annual NO_3^- discharge and NH_3 emissions modelled from 16 Sep. to 15 Sep. in 2014/2015 and 2015/2016 without slurry (C) or with slurry applied in fall (F) or spring (S) without NI and with DMPP on dates in the field study (Table 3), and in fall on dates 2 weeks before (F-2) or after (F+2) those in the field study, and with soil mixing during slurry application (M) increased to 0.5 and 0.8 from 0.2 in the field study. For NH_3 positive values indicate deposition, negative values emission.

	Year	2014/5		2015/6	
Treat.	Amend.				
		NH_3	NO_3^-	NH_3	NO_3^-
		---------- mg N m^{-2} ----------			
C		+14	277	+34	421
F	none	+7	330	+29	691
F	DMPP	-147	317	+13	662
S	none	+8	279	+21	617
S	DMPP	+4	279	+14	598
F -2	none	+4	336	+26	678
F -2	DMPP	-9	326	+12	658
F +2	none	+3	336	+28	697
F +2	DMPP	-194	321	+10	662
F 0.5	none	-9	321	+17	558
F 0.5	DMPP	-79	314	-3	554
F 0.8	none	-34	500	+1	368
F 0.8	DMPP	-101	473	-29	370
S 0.5	none	-3	279	+1	490
S 0.5	DMPP	-7	279	-8	493
S 0.8	none	-15	279	-15	361
S 0.8	DMPP	-21	279	-26	365

Table 8: Barley silage yields modelled and measured without slurry (C) or with slurry applied in fall (F) or spring (S) with and without NI applied on dates in the field study (Table 3)

	Year	2015		2016	
Treat.	Amend.				
		Mod.	Mes. †	Mod.	Mes. †‡
		---------- g C m^{-2} ----------			
C		154	198 ± 24	128	124 ± 9
F	none	284	355 ± 4	344	242 ± 45
F	DMPP	283	360 ± 25	343	255 ± 15
S	none	293	267 ± 12	334	195 ± 33
S	DMPP	297	317 ± 17	344	189 ± 32

† calculated as 45% DM

‡ measured yields reduced by lodging

Table 9: Sensitivity of seasonal N_2O emissions modelled during late spring in 2015 and 2016 to changes in initial inhibition ($I_{t=0}$ in Eq. 1) and inhibition constant (K_{iNH4} in Eq. 2) following spring slurry application on dates in the field study (Table 3). Negative values denote emissions.

Year		2015	2016
Period		12 May – 11 June	17 May – 16 June
		---------- mg N m^{-2} --------	
No NI		-89‡	-153‡
$I_{t=0}$	K_{iNH4}		
1.0	7000	-58‡	-72‡
0.9	7000	-60	-80
0.8	7000	-62	-90
1.0	3500	-62	-78
0.9	3500	-64	-86
0.8	3500	-65	-95
1.0	14000	-54	-66
0.9	14000	-57	-75
0.8	14000	-59	-85

‡ from Table 5

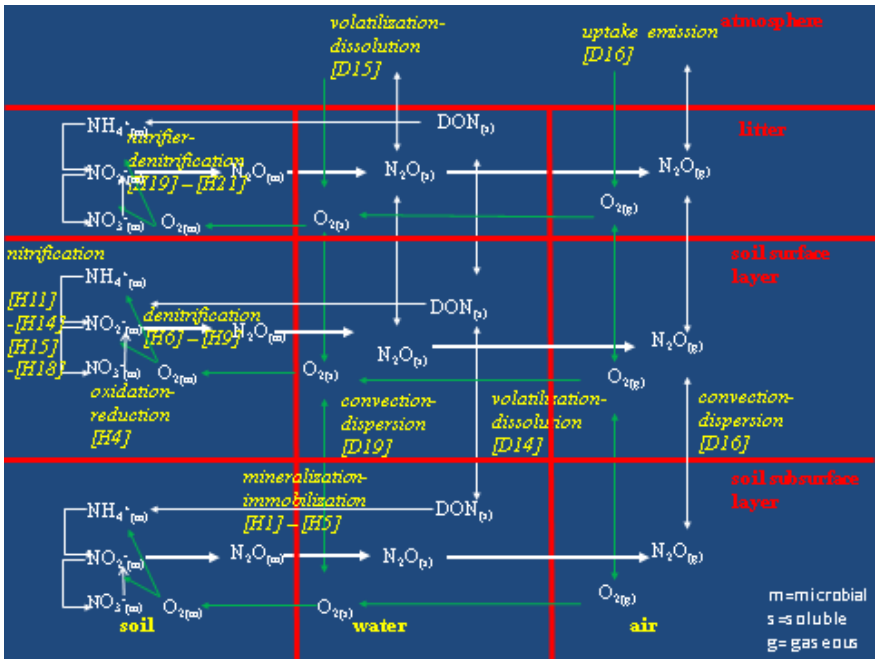

Fig. 1. Key transformations governing N_2O emissions as represented in *ecosys*. Expressions in square brackets refer to equations in the Supplement as described in Sec. 2.

1324

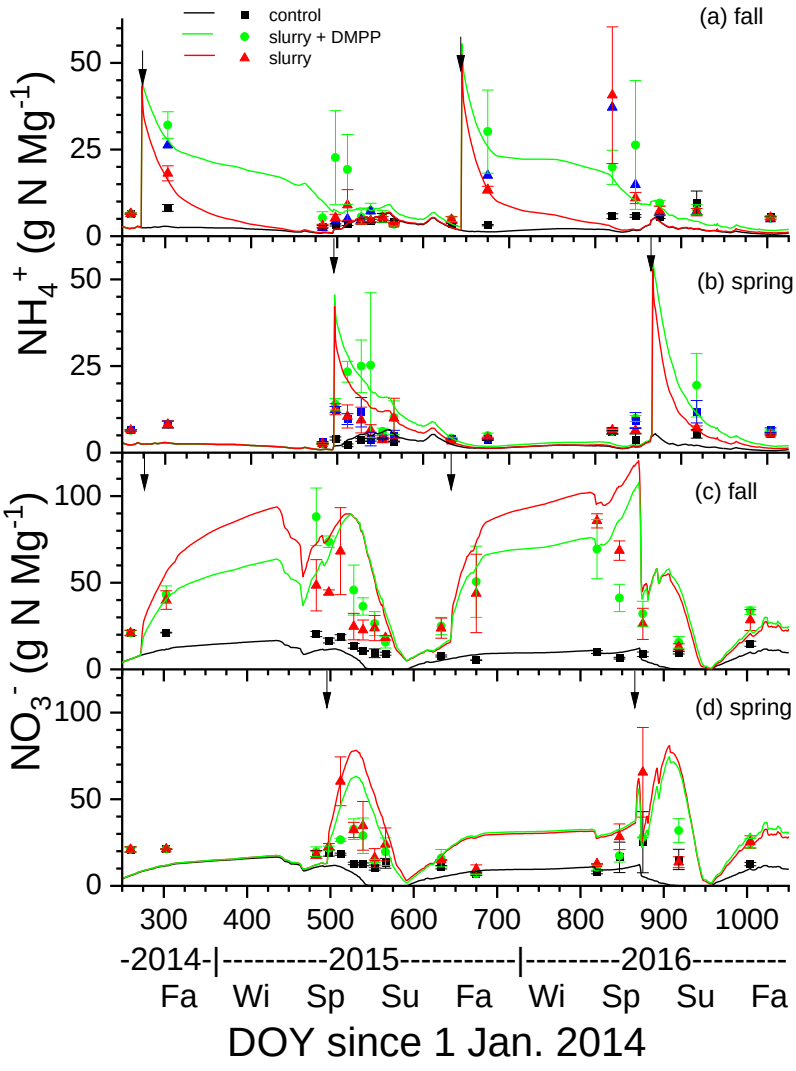
control
slurry + DMPP
slurry
(a) fall
(b) spring
(c) fall
(d) spring
NH4+ (g N Mg-1)
NO3- (g N Mg-1)
0
25
50
100
300
400
500
600
700
800
900
1000
-2014-|----------2015----------|---------2016---------
Fa Wi Sp Su Fa Wi Sp Su Fa
DOY since 1 Jan. 2014

1325

Fig. 2. Soil NH_4^+ and NO_3^- concentrations measured (symbols) and modelled (lines) at 0 – 10 cm depth following applications of dairy slurry without and with DMPP. Arrows indicate dates of application.

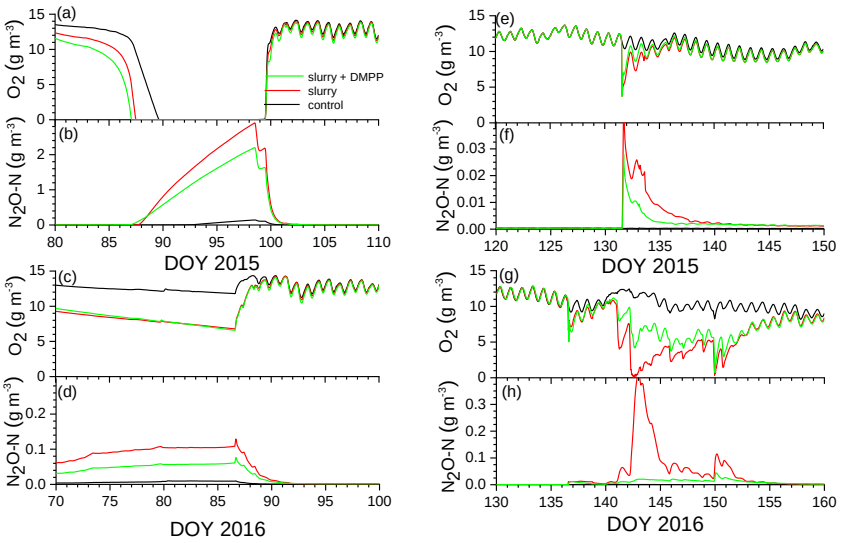

Fig. 3. Aqueous concentrations of O_2 and N_2O modelled at depth of slurry injection (14 cm) during emission events in early spring of (a,b) 2015 and (c,d) 2016 after fall slurry applications with or without DMPP on DOY 273 in 2014 and DOY 280 in 2015, and in later spring of (e,f) 2015 and (g,h) 2016 after spring slurry applications on DOY 132 in 2015 and DOY 137 in 2016.

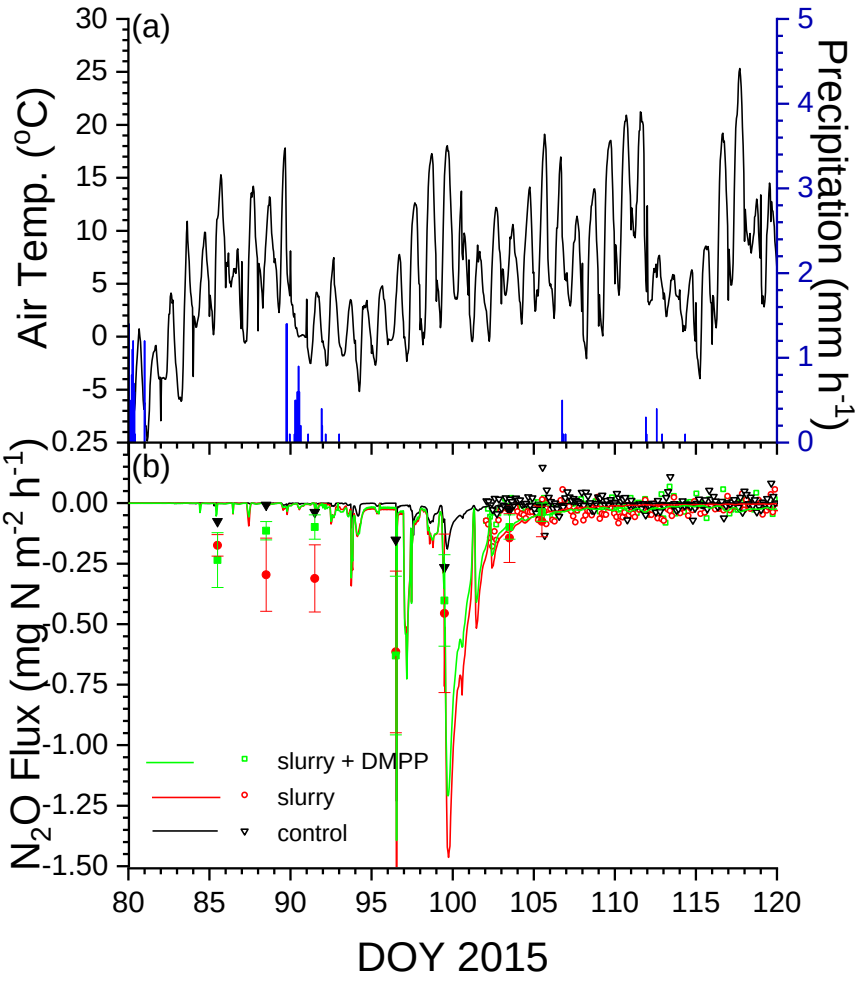

Fig. 4. (a) Air temperature and precipitation, and (b) N_2O fluxes measured (symbols) and modelled (lines) during early spring 2015 with no slurry (control), and following slurry application on DOY 273 in 2014 with or without DMPP. Filled symbols represent manual chamber measurements by Lin et al. (2018). Negative values denote emissions.

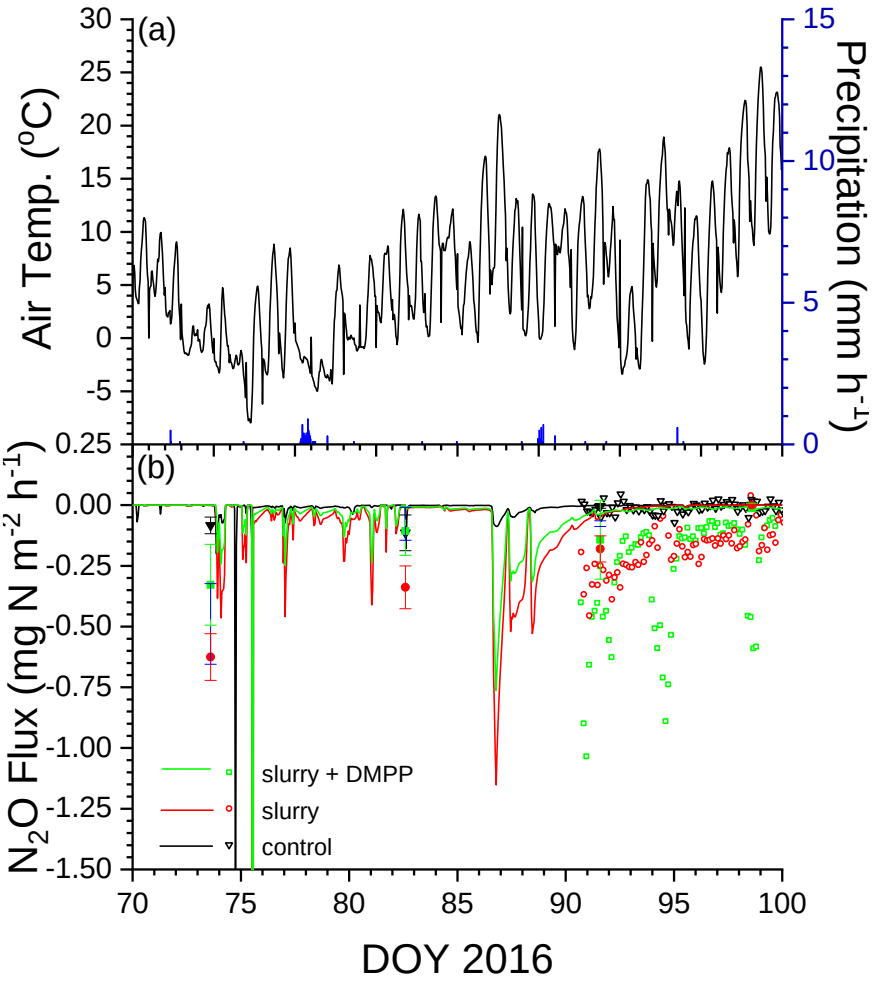

1339

1340 **Fig. 5**. (a) Air temperature and precipitation, and (b) N_2O fluxes measured (symbols) and
1341 modelled (lines) during early spring 2016 with no slurry (control), and following slurry
1342 application on DOY 280 in 2015 with or without DMPP. Filled symbols represent manual
1343 chamber measurements. Negative values denote emissions.

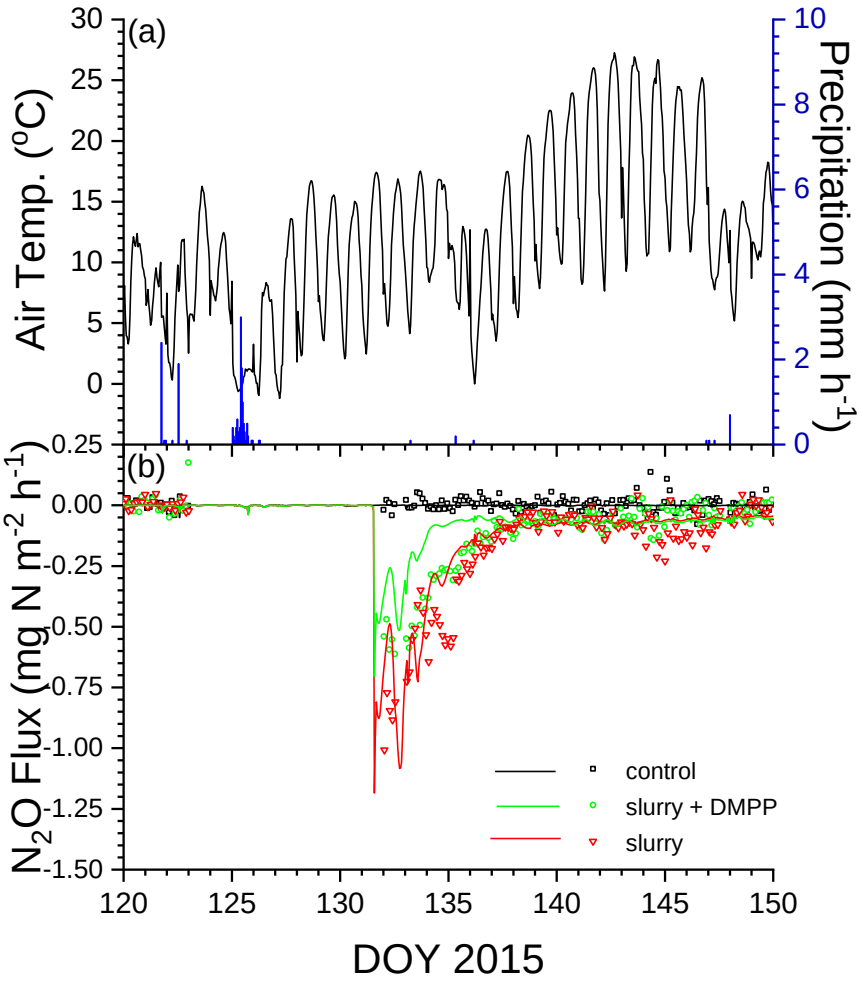

Fig. 6. (a) Air temperature and precipitation, and (b) N_2O fluxes measured (symbols) and modelled (lines) during spring 2015 with no slurry (control), and following slurry application on DOY 132 in 2015 with or without DMPP. Negative values denote emissions.

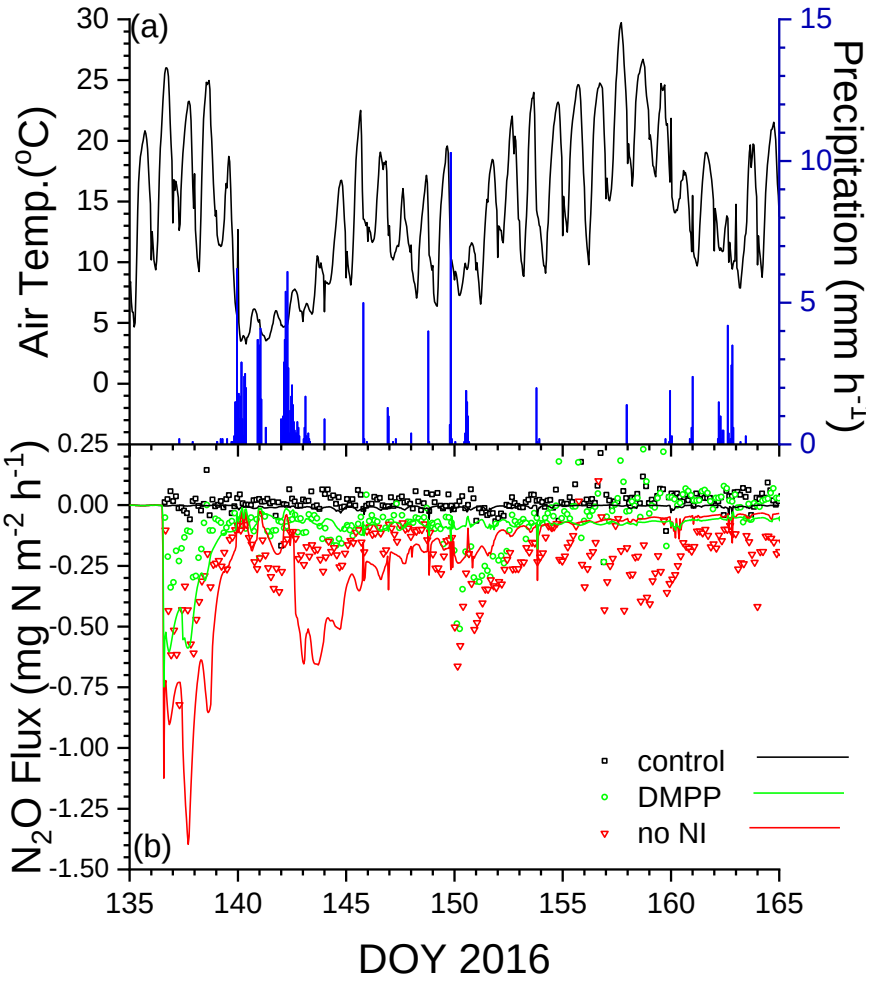

1349

1350 **Fig. 7**. (a) Air temperature and precipitation, and (b) N_2O fluxes measured (symbols) and
1351 modelled (lines) during spring 2016 with no slurry (control), and following slurry application on
1352 DOY 137 in 2016 with or without DMPP. Negative values denote emissions.

1353